ELSEVIER

Journal of Neuroimmunology 190 (2007) 90–100

Journal of
Neuroimmunology

www.elsevier.com/locate/jneuroim

Characterization of pathogenic T cells and autoantibodies in C-protein-induced autoimmune polymyositis

Yoh Matsumoto *, Kuniko Kohyama, Il-Kwon Park, Mie Nakajima, Keiko Hiraki

Department of Molecular Neuropathology, Tokyo Metropolitan Institute for Neuroscience, Musashidai 2-6, Fuchu, Tokyo 183-8526, Japan

Received 1 August 2007; received in revised form 27 August 2007; accepted 27 August 2007

Abstract

Although autoimmune processes may take place in human polymyositis, little is known with regard to its pathogenesis due to the lack of appropriate animal models. In the present study, we developed experimental autoimmune myositis (EAM) in Lewis rats by immunization with recombinant skeletal C-protein and examined the role of pathogenic T cells and autoantibodies. Using recombinant proteins and synthetic peptides, we demonstrated that skeletal C-protein Fragment 2 (SC2) has the strongest myositis-inducing ability and that myositis-inducing epitope(s) reside within the residues 334–363 of SC2 (SC2P3). However, immunization with SC2P3 induced only mild EAM compared with SC2 immunization. Characterization of T cells and antisera revealed that SC2P3 and SC2P7 contain the B cell epitope, while the T cell epitope resides in SC2P5. Furthermore, anti-SC2, but not anti-SC2P3, antisera contained antibodies against the conformational epitope(s) in the SC2 molecule. However, SC2P3 or SC2P5 immunization plus anti-SC2 antibody transfer aggravated the disease only slightly. These findings suggest that C-protein-induced EAM is formed by activation of C-protein-specific T cells along with antibodies against conformational epitopes in C-protein but that there are undetermined factors related to the disease progression. Further analysis of C-protein-induced EAM will provide useful information to elucidate the pathomechanisms of human polymyositis.

Keywords: Experimental autoimmune myositis; Lewis rat; Protein; Myosin; Immunohistochemistry; B cell epitopes

1. Introduction

Human polymyositis (PM) is a disorder of skeletal muscle characterized by lymphocyte infiltration into the muscle. Immunohistochemical studies of skeletal muscle revealed that T cells are a predominant population of infiltrating inflammatory cells. While CD4-positive T cells were abundant among the surrounding cells, CD8-positive T cells were major invading cells (Arahata and Engel, 1984; Dalakas, 1992; Engel and Arahata, 1984). These findings suggest that PM is an autoimmune disease. However, little is known regarding its pathogenesis partly because a good animal model for PM is not available at present. In previous studies, we and others induced experimental autoimmune polymyositis (EAM) in Lewis rats by immunization with partially purified skeletal myosin (Kojima et al., 1997; Nemoto et al., 2003). During the process of subsequent investigations, we found that immunization with myosin that had been further purified from partially purified myosin preparations induced only mild EAM compared with partially purified myosin-induced EAM. Moreover, immunization with purified C-protein, a myosin-binding protein (Offer, 1972; Offer et al., 1973), induced severe EAM of high histological grade and lesion frequency comparable with EAM induced with partially purified myosin. These findings suggested that C-protein is the major myositogenic antigen that exists in the partially purified myosin preparation (Kohyama and Matsumoto, 1999).

C-protein is a single polypeptide chain of approximately 140 kDa, which is present in thick filaments of skeletal and cardiac muscles. It binds to myosin rods, light meromyosin, and F-actin (Dennis et al., 1984). Although its function is not fully

Abbreviations: EAM, experimental autoimmune myositis; PM, polymyositis; SC2, skeletal muscle C-protein fragment 2; SC2P3, SC2 peptide 3.

* Corresponding author. Tel.: +81 423 25 3881x4719; fax: +81 423 21 8678.
E-mail address: matyoh@tmin.ac.jp (Y. Matsumoto).

0165-5728/$ - see front matter © 2007 Elsevier B.V. All rights reserved.
doi:10.1016/j.jneuroim.2007.08.013

understood, C-protein seems to encircle each thick filament and to play an important role in stabilizing the thick filament structure (Fischman et al., 1991). C-protein is a member of the immunoglobulin super family and has several isoforms and different isoforms have characteristic distributions (Dennis et al., 1984).

Analysis of EAM using native C-protein purified from skeletal muscle has several limitations. Firstly, C-protein comprises only 2% of muscle proteins and therefore it is difficult to perform experiments using a large amount of the protein (Offer, 1972; Offer et al., 1973). Secondly, further investigation with native C-protein revealed that the purity and myositogenicity of the protein varied greatly from lot to lot, resulting in variation in the induction of EAM. Finally and most importantly, fine specificity analysis was difficult due to its large molecular size.

To overcome these problems, we have prepared, in the present study, recombinant skeletal C-protein fragments (SC1–SC4) and overlapping synthetic peptides corresponding to one of the fragments (SC2). Analysis of the T and B cell epitopes revealed that the T epitope resides within peptides 5 (SC2P5), whereas anti-SC2 antibodies react with SC2P3 and SC2P7. Furthermore, it was suggested that full-blown EAM is induced by synergistic effects by T cells and antibodies responding these epitopes. Thus, the animal model established in the present study will provide useful information to analyze the pathomechanisms and to develop specific immunotherapy for human PM.

2. Materials and methods

2.1. Animals

Lewis rats were purchased from SLC Japan (Shizuoka) and bred in our animal facility. Rats used in the present study were 8–12 weeks old. All the experiments performed in the present study were approved by Ethical Committee of Tokyo Metropolitan Institute for Neuroscience.

2.2. C-protein purification

C-protein was isolated from partially purified myosin. The C-protein-containing fraction was concentrated and dialyzed against 0.3 M KCl, 0.01 M potassium phosphate (pH 7.0) with 0.01% sodium azide. Hydroxyapatite column chromatography was performed according to Starr and Offer (1982) with a few modifications. The sample was applied to a 1.6×15 cm column of hydroxyapatite (Calbiochem, Tokyo, Japan) and eluted with potassium phosphate pH7.0 (0.01–0.5 M linear gradient) to obtain purified C-protein, which was present in approximately 0.15 M potassium phosphate.

Detection of C-protein was performed by polyacrylamide gel electrophoresis, which revealed the protein as a band of about 140 kDa. This was also confirmed by western blotting with anti-C-protein mAb. To determine the purity of C-protein obtained, 1 μg of the protein was run on a gradient PAGE (5–20%) (Biocraft, Tokyo, Japan) and the gel was stained with SYPRO Red (Molecular Probes, Eugene, OR) for 30 min. Then, the profiles were recorded using an FMBIO II fluorescence image analyzer (Hitachi, Yokohama, Japan). The percentage of C-protein was calculated as the percentage of the density of a band of 140 kDa per the density of the total protein.

2.3. Preparation of recombinant C-protein fragments

Since C-protein (140 kDa) is too large to prepare the recombinant protein as a whole protein, we planned to produce four protein fragments designated as Fragments 1, 2, 3, and 4 as shown in Fig. 1. Total RNA was isolated from human psoas muscle using RNAzol B (Biotecx Laboratories, Houston, TX)

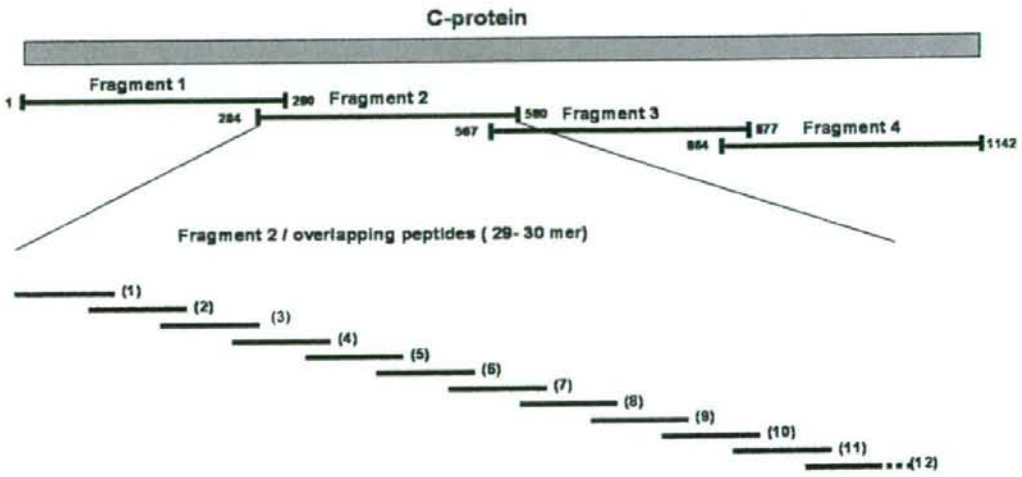

Fig. 1. Recombinant C-protein and synthetic peptides used in this study. Four recombinant protein fragments corresponding to residues 1–290, 284–580, 567–877 and 864–1142 of C-protein were prepared from transformed *E. coli* and purified with an affinity column. Twelve overlapping 29–30 mer synthetic peptides covering Fragment 2 were also prepared for immunization and in vitro proliferation assay.

and then reverse transcribed into cDNA using ReverTra Ace-α- (TOYOBO, Osaka, Japan). Then, cDNA was amplified by PCR with KOD DNA polymerase (TOYOBO) and fragment-specific primer pairs. Primers used in this study were as follows: Fragment 1 (sense primer=5′-GAGAGGTACCATGCCT-GAGGCAAAACCAGCG-3′, antisense primer=5′-GAGAGTCGACTCAGAACCACTTGAGGGTCAGGTC-3′); Fragment 2 (sense primer=5′-GAGAGGATCCGACCT-GACCCTCAAGTGGTTC-3′, antisense primer=5′-GAGAAA-GCTTCAGCCAGGTAGCGACGGGAGG-3′); Fragment 3 (sense primer=5′-AGAGGATCCCCTCCCGTCGCTACCT-GGCTG-3′, antisense primer=5′-AGAAAGCTTCC-GGGGCTTTCCCTGGAAGGG-3′) and, Fragment 4 (sense primer=5′-AGAGGATCCCCCTTCCAGGGAAAGCCCCGG-3′, antisense primer=5′-AGAAAGCTTTCACTGCGG-CACTCGGACCTC-3′). Each primer was designed to introduce the restriction enzyme sites at both ends. PCR products were inserted into a cloning vector, pCR4 Blunt-TOPO in the Zero Blunt TOPO kit (Invitrogen, CH Groningen, the Netherlands), and clones with the correct sequences were obtained by the standard method. Several clones were subcloned into an expression vector, pQE30 (QIAGEN, Tokyo, Japan), and used for large-scale preparation of C-protein fragments. Recombinant C-protein fragments produced in transformed *E. coli* were isolated under denaturing conditions and purified using Ni-NTA Agarose (QIAGEN). Then, purified protein fragments were refolded in 100 mM PBS containing 500 mM L-arginine, 2 mM glutathione (reduced form), 0.2 mM glutathione (oxidized form), and 2 mM EDTA. As a final step, recombinant protein fragments were incubated with Detoxi-Gel (PIERCE, Funakoshi, Tokyo, Japan) overnight to remove endotoxins. Obtained protein fragments contained endotoxins less than 10 EU/1 mg protein as determined with Toxinometer ET-2000 (Wako, Tokyo, Japan).

Overlapping 29–30 mer synthetic peptides covering C-protein Fragment 2 (SC2) were synthesized using a peptide synthesizer (PSSM-8, Shimadzu, Kyoto, Japan) and designated as SC2P1-P12 (Fig. 1). All the peptides used in this study were >90% pure, as determined, and purified if necessary, by HPLC.

2.4. EAM induction and tissue sampling

Lewis rats were immunized by intramuscular injections of the indicated antigen with complete Freund adjuvant (CFA) (Gibco, Tokyo, Japan) in multiple sites of the back three times on a weekly basis, and were sacrificed two weeks after the last immunization. For controls, PBS/CFA was injected according to the same protocol. Where indicated, *M. tuberculosis* (Gibco) was further supplemented to 5 mg/ml (5CFA). To prevent degeneration of the antigens, only freshly prepared or short-term preserved (one month or less at −80 °C) preparations were used for experiments. At the time of immunization, rats received an intraperitoneal injection of 2 μg pertussis toxin (PT) (Seikagakukogyo, Tokyo, Japan). Histological and immunohistochemical examinations were performed using frozen sections of muscle that had been removed from a proximal part of lower extremities (total six blocks) and snap frozen in chilled isopentane precooled in liquid nitrogen.

2.5. Histological grading of inflammatory lesions and immunohistochemistry

Using hematoxylin and eosin-stained sections, histological severity of inflammation was graded into four categories: grade 1, single or less than 5 muscle fiber involvement; grade 2, a lesion involving 5–30 muscle fibers; grade 3, a lesion involving a muscle fasciculus; grade 4, a diffuse extensive lesion. When multiple lesions were found in one muscle block, 0.5 was added to the score.

ATPase staining was performed to distinguish fast (white) muscle fibers from slow (red) muscle fibers. Frozen sections were treated with barbital acetate solution, 0.1 M HCl (pH 4.6) for 5 min after which the sections were washed in 0.1 M sodium barbital, 0.18 M $CaCl_2$ (pH 9.5). Then, sections were reacted with ATP disodium salt in sodium barbital solution for 45 min. The reaction products were visualized in 1% ammonium sulfide solution (yellow).

Immunoperoxidase staining was performed as described (Matsumoto et al., 1986). Briefly, frozen sections, 10 μm thick, were air-dried and fixed in ether for 10 min. After incubation with normal sheep serum, sections were allowed to react with mAb, biotinylated horse anti-mouse Ig (1:200) (Vector, Burlingame, CA) and horseradish peroxidase (HRP)-labeled VECTASTAIN® *Elite* ABC Kit (Vector). HRP-binding sites were detected using a Sigma Fast DAB Tablet set (Sigma). The monoclonal antibodies (mAb) in the present study were R73 (1:800) (anti-T cell receptor αβ), OX42 (1:400) (anti-macrophage), W3/25 (1:400) (anti-CD4), and clone 341 (1:200) (anti-CD8). The mAbs were purchased from Serotec (Blackthorn, Bicestor, Bucks, UK) or purified from culture supernatant of hybridomas. Immunohistochemical staining with anti-SC2 mAbs, which were raised using recombinant SC2 protein, was also performed to test whether the mAbs react with native protein. To confirm the specificity, the mAbs were absorbed by incubating with 10 M excess of recombinant SC2 for 1 h at 37 °C and immunohistochemistry was performed.

2.6. Proliferative responses of T cells against SC2 and SC2 peptides

Proliferative responses of lymph node cells were assayed in microtiter wells by uptake of $\{^3H\}$-thymidine. After being washed with PBS, lymph node cells (2×10 cells/well) were cultured with the indicated concentrations of SC2 or SC2 peptides for 3 days, with the last 18 h in the presence of 0.5 μ Ci $\{^3H\}$ thymidine (Amersham Pharmacia Biotech, Tokyo). In some experiments, the proliferative responses of SC2 or SC2 peptide-specific T line cells (3×10^4 cells/well) were assayed in the presence of the antigens and APC (5×10^5 cells/well). The cells were harvested on glass-fiber filters, and the label uptake was determined using standard liquid scintillation techniques.

2.7. ELISA and western blot analysis

The levels of anti-SC2 and anti-SC2 peptide antibodies were measured by ELISA. Recombinant SC2 and SC2 peptides

Table 1
Induction of experimental autoimmune myositis with native C-protein preparations

Immunization[a]		Incidence[b]	% inflammatory lesion[c]	Histological score[d]
Native C-protein	Purity[e]			
Lot #6	52%	7/7	35/42 (83%)	1.9±1.0
Lot #7	68%	3/8	8/48 (17%)	0.9±0.4
Lot #8	42%	3/4	7/24 (29%)	0.9±0.4
Lot #9	38%	3/3	12/18 (67%)	1.0±0.2

[a] Lewis rats were immunized with the indicated lot of native C-protein in CFA along with pertussis toxin and sacrificed one week after the last immunization. Muscles in the hind feet were removed (6 blocks) and snap frozen in chilled isopentane. Histological severities were graded in four categories: grade 1, single or less than 5 lesions involving 1–5 muscle fiber(s); grade 2, single lesion involving 5–30 muscle fibers or single muscle fasciculus; grade 3, single lesion involving 1–10 muscle fasciculus; grade 4, a diffuse extensive lesion.

[b] When inflammation was found in at least one site on hematoxylin and eosin-stained sections, rats were scored as positive.

[c] No. of muscle blocks containing inflammatory foci/No. of total blocks examined.

[d] Total histological scores/No. of blocks examined±SE.

[e] The purity of each C-protein preparation was determined as follows. Each lot of C-protein was run on a gradient PAGE and stained with SYPRO Red. Then, the profiles were recorded using an FMBIO II fluorescence image analyzer. The percentage of C-protein was calculated as the percentage of the density of a band of 140 kDa per the density of the total protein.

(10 μg/ml) were coated onto microtiter plates and serially diluted sera from normal and immunized animals were applied. After washing, appropriately diluted horseradish-conjugated anti-rat IgG, IgG1, or IgG2a was applied. The reaction products were then visualized after incubation with the substrate. The absorbance was read at 450 nm.

For the immunoblot assay, SC2 was run on a 10% SDS-PAGE gel and immunoblotted onto nitrocellulose membrane (Bio-Rad, Hercules, CA). The residual binding sites on the membrane were blocked by incubation with 5% nonfat milk in TBS buffer (10 mM Tris–HCl, pH 7.4, and 150 mM NaCl) for 1 h and then incubated with anti-SC2 mAb for 2 h. The blots were washed three times in TBS containing 0.1% Tween-20, probed with horseradish peroxidase-conjugated anti-mouse IgG (New England Biolabs, Inc, Beverly, MA) for 1 h. The blots were developed by enhanced chemiluminescence reagents (Amersham Life Science, Arlington Heights, IL) according to the manufacturer's instructions. The density of each band obtained by western blot analysis was measured with a scanning laser densitometer (GS-700, Bio-Rad, Hercules, CA) and analyzed using Molecular Analyst software (Bio-Rad, Hercules, CA).

2.8. Purification of sera with SC2- or SC2 peptide-coupled column

SC2- or SC2 peptide-coupled affinity columns were prepared using HiTrap NHS-activated columns (GE Healthcare, Bioscience Corp, Tokyo, Japan) according to the manufacturer's instructions. SC2 was dialyzed in the standard coupling buffer (0.2 M $NaHCO_3$, 0.5 M NaCl, pH 8.3) and the SC2 peptide mixture (SC2P1–SC2P12) was dissolved in dH_2O containing 1% DMSO and 1% PBS. SC2 or peptide mixture was coupled to the column as a ligand. Then, sera obtained from EAM-induced rats were fractionated on SC2- or SC2 peptides-coupled columns. Briefly, the sera were diluted five-fold with PBS and applied to the column that had been equilibrated with 20 mM $Na–PO_4$, pH 7. After the flowthrough was saved, the column was washed and the bound protein was eluted with 0.1 M glycine–HCl, pH 2.7 and immediately neutralized with 1 M Tris–HCl, pH 9. The levels of anti-SC2 and anti-SC2 peptide antibodies in the flowthrough and eluate were determined by ELISA.

2.9. Generation of monoclonal and polyclonal antibodies against SC2 and SC2 peptides and transfer experiments

Anti-SC2 and anti-SC2P3 mAbs were generated by immunizing Balb/C mice (SLC, Shizuoka, Japan) with SC2 and SC2P3, respectively. To increase the immunogenicity of SC2P3, the peptide was conjugated with keyhole limpet hemocyanin (KLH) (Wako, Tokyo, Japan) before use. Mice were first immunized with 50 μg antigens emulsified with CFA followed by intraperitoneal injections of antigens/IFA in a total of six times. The sufficient production of antibodies was confirmed by ELISA using sera obtained by retro-orbital puncture. After the final boost, spleen cells taken from immunized mice were hybridized with myeloma cells (X63Ag8.653) using polyethylene glycol (PEG/DMSO solution Hybri-Max, Sigma, Tokyo, Japan). After seeding onto microplates, hybridoma cells were selected in the HAT medium. Ten to fourteen days later, antibody-producing cells were screened by ELISA and cloned by limiting dilution. Established clones were expanded in culture and cells were injected intraperitoneally to Balb/C mice with Pristane (Sigma) to obtain a large amount of mAbs. The mAbs obtained was purified on a HiTrap protein G column (Amersham Bioscience, Tokyo, Japan). Anti-SC2 rat mAbs were also generated in a similar way. In this case, Lewis rats were immunized with SC2 and sacrificed 2 weeks

Table 2
Histological severities of EAM induced by immunization with recombinant skeletal C-protein fragments[a]

Antigen	Incidence[b]	% inflammatory lesion[c]	Mean histological score[d]
SC1	4/4	13/24 (63%)	0.83±0.20
SC2	9/9	35/54(65%)	1.36±0.18
SC3	6/6	17/35 (51%)	1.09±0.23
SC4	2/3	6/18 (39%)	0.56±0.20
PBS	2/3	2/19 (11%)	0.11±0.08

a) Lewis rats were immunized with recombinant C-protein fragment 1, 2, 3, or 4 (SC1, SC2, SC3 and SC4, respectively) in CFA along with pertussis toxin and sacrificed one week after the last immunization. PBS/CFA-immunized controls showed non-specific single muscle fiber necrosis in two of three rats. Therefore, such finding was not judged as positive in SC-immunized animals.

b) When inflammation was found in at least one site on hematoxylin and eosin-stained sections, rats were scored as positive.

c) No. of muscle blocks containing inflammatory foci/No. of total blocks examined.

d) Total histological scores/No. of blocks examined±SE.

e) Significantly different between SC1 and PBS ($p<0.01$), between SC2 and PBS ($p<0.001$), between SC3 and PBS ($p<0.01$), and between SC4 and PBS ($p<0.05$) by Student's t test.

after immunization. Iliac lymph node cells were taken from the rats and hybridized with myeloma cells, SP2/0-Ag14, kindly provided by Dr. Sado (Shigei Medical Research Institute, Okayama, Japan).

Polyclonal antibodies against SC2 and SC2 peptides were raised by immunizing rats with the antigens/CFA four times on a weekly basis. Sera were obtained one week after the last immunization and ammonium sulfate-precipitated preparations were used for the transfer experiments. The presence of antibodies against the indicated antigens was confirmed by ELISA.

For the transfer experiments, rats were first immunized with SC2 peptide and the indicated doses of sera or mAb were injected intravenously twice a week for 3 weeks. Rats were examined histologically 2 weeks after the last antibody administration.

2.10. Statistical analysis

Unless otherwise indicated, Student's t test or Mann–Whitney's U-test was used for the statistical analysis.

3. Results

3.1. Purity and myositogenicity of native C-protein purified from skeletal muscle varied from lot to lot of the protein

In a previous report (Kohyama and Matsumoto, 1999), we showed that immunization with purified native C-protein induced severe EAM in Lewis rats comparable with that induced with partially purified skeletal myosin (Kojima et al.,

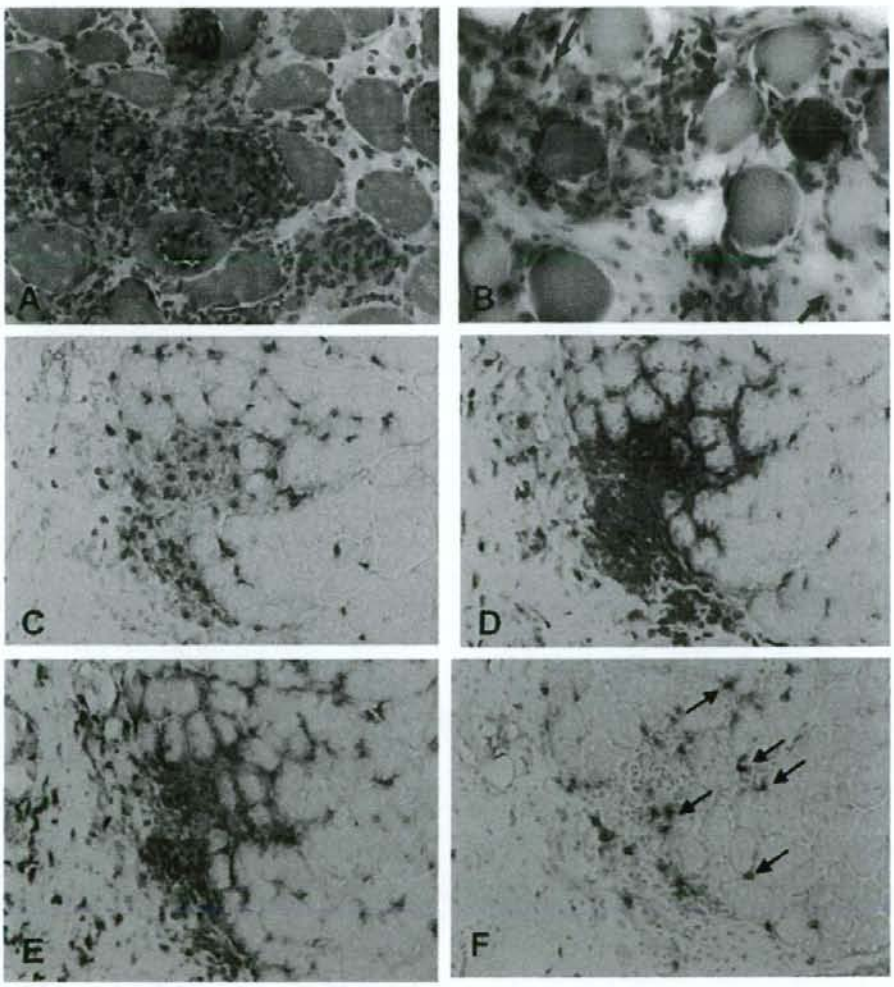

Fig. 2. Immunopathology of C-protein-induced EAM. In H and E staining (A), inflammatory cells infiltrated muscle fibers (one of the residual fibers is indicated by arrow heads) and the perimysial space is filled with infiltrating cells. ATPase staining (B) revealed that white muscle fibers (light staining and indicated by arrows) are attacked by inflammatory cells, whereas red muscle fibers (dark staining and indicated by arrow heads) are relatively spared from inflammation. Immunoperoxidase staining demonstrated that TCR αβ-positive T cells (C) and macrophages (D) have mainly infiltrated the lesion. Although CD4-positive cells (E) outnumber CD8-positive cells (F), CD8-positive cells infiltrated the muscle fibers (arrows in F).

1997). In contrast, highly purified myosin induced only mild EAM. These findings suggested that the major myositogenic component in the partially purified myosin preparation is C-protein. To characterize C-protein-induced EAM in more detail, we repeated the experiments using new lots of native C-protein. Unexpectedly, however, the purity and myositogenicity of purified native protein varied from lot to lot, as summarized in Table 1. All the rats (7 out of 7) that had received Lot #6 developed severe EAM with a mean histological score of 1.9 in 35 muscle blocks out of 42 blocks examined. In contrast, Lots #7 and #8 induced only mild EAM with histological scores of 0.9 in 17–29% of muscle sections. It should be noted that the purity of C-protein in each lot did not always correlate with myositogenicity. For instance, Lot #7 with relatively high purity (68%) induced mild EAM, while Lot #9 with low purity (38%) induced intermediate EAM (Table 1). This was probably because myositogenicity of purified native C-protein is related not only to the purity of C-protein, but also to the preservation of the intact protein after purification.

3.2. *Incidence and immunopathology of recombinant C-protein-induced EAM*

To overcome the above problems and to obtain a sufficient amount of C-protein with high purity, we decided to prepare recombinant proteins. Since C-protein is too large to produce a plasmid encoding the whole sequence of the protein, we prepared four plasmids encoding four parts of fast-type C-protein as shown in Fig. 1. Fragments 1, 2, 3, and 4 (referred to as SC1, SC2, SC3, and SC4) correspond to residues 1–290, 284–580, 567–877, and 864–1142, respectively. Then, purified recombinant protein fragments were immunized three times on a weekly base into Lewis rats, and muscle blocks were taken two weeks after the last immunization for histological examination. The results are summarized in Table 2. Immunization with SC1, SC2, SC3, and SC4 induced EAM in all rats. Control rats that were immunized with PBS/CFA showed mild non-specific inflammation in the muscle with very low incidence compared with C-protein-immunized rats (Table 2). We have checked the site of inflammation in PBS/CFA-immunized rats and found that inflammation was far from the immunization site. Therefore, it is unlikely that inflammation was tissue damage directly induced by adjuvant. Among the C-protein-immunized groups, SC2 induced severe EAM with mean histological severity of 1.36±0.18 in 65% of muscle tissue blocks comparable with partially purified myosin-induced or native C-protein-induced EAM (Kohyama and Matsumoto, 1999). Similarly, SC3 induced intermediate EAM. Immunization with SC1 and SC4 resulted in relatively mild EAM in terms of incidence and severity. These findings indicate that in the C-protein molecule, there are multiple myositis-inducing epitopes.

Histological examination revealed severe inflammatory cell infiltration into muscle fibers (Fig. 2A). In ATPase staining, inflammatory cells comprising T cells and macrophages mainly infiltrated fast-type fibers (Fig. 2B, arrows) and slow-type fibers

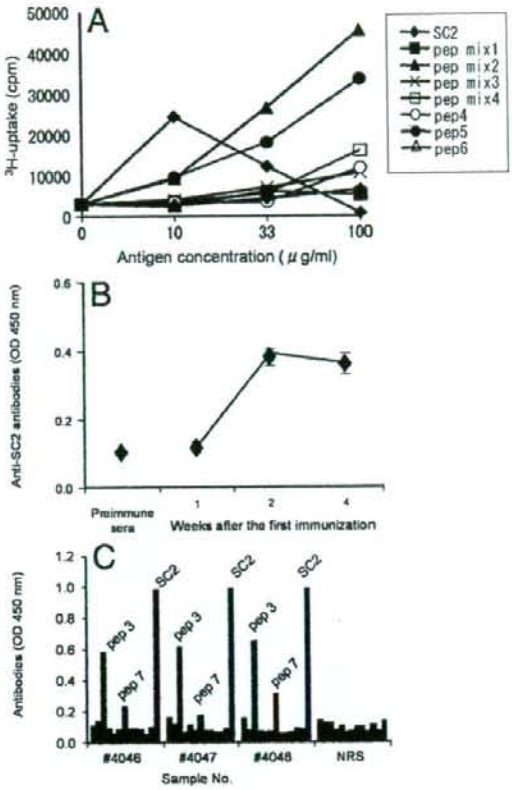

Fig. 3. Characterization of T cells and autoantibodies in SC2-induced EAM. A; Proliferative responses of lymph node cells taken from SC2-immunizaed rats respond vigorously to Mix 2 (SC2P4, P5 and P6, closed triangles) and pep5 (SC2P5, closed circles). Lymph node cells also react with the immunogen, SC2 (closed diamonds). B; Kinetics of anti-SC2 antibody titer during the course of EAM. The level of anti-SC2 antibodies increased and reached a maximum two weeks after the first immunization. Sera were taken from the same animals at various time points. C; The reactivities of anti-SC2 antisera to overlapping synthetic peptides encompassing SC2. All the sera taken from SC2-immunized rats 4 weeks after the first immunization reacted with peptide 3 (SC2P3) and, to lesser extent, to peptide 7 (SC2P7). NRS, normal rat serum.

Table 3
Sequences of SC2[a] peptides used in the study

Peptide	Residue	Sequence
SC2P1	SC284–313	DLTLKWFKNGQEIKPSSKYVFENVGKKRIL
SC2P2	SC309–338	KKRILTINKCTLADDAAYEVAAYEVKCFTE
SC2P3	SC334–363	KCFTELFVKEPPVLIVTPLEDQQVFVGDRV
SC2P4	SC359–388	VGDRVEMAVEVSEEGAQVMWMKDGVELTRE
SC2P5	SC384–412	ELTREDSFKARYRFKKDGKRHILIFSDVV
SC2P6	SC408–436	FSDVVQEDRGRYQVITNGGQCEAELIVEE
SC2P7	SC432–460	LIVEEKQLEVLQDIADLTVKASEQAVFKC
SC2P8	SC456–484	AVFKCEVSDEKVTGKWYKNGVEVRPSKRI
SC2P9	SC480–508	PSKRITISHVGRFHKLVIDDVRPEDEGDY
SC2P10	SC504–532	DEGDYTFVPDGYALGSLSAKLNFLEIKVE
SC2P11	SC528–556	EIKVEYVPKQEPPKIHLDCSGKTSENAIV
SC2P12	SC552–572[b]	ENAIVVVAGNKLRLDVSITGE

[a] Amino acid residues 284–580 of human skeletal C-protein, fast type.
[b] Amino acid residues 573–580 (PPPVATWL) were deleted because the sequence was difficult to synthesize.

Table 4
Histological severities of EAM induced by immunization with synthetic peptides[a]

Group	Antigen	Dose (μg)	Incidence[b]	% inflammatory lesion[c]	Mean histological score[d]
A	SC2	100/cCFA[e]	9/9	35/54 (65%)	1.36±0.18[f]
B	SC2P1	100/cCFA	2/3	3/18 (17%)	0.17±0.09
C	SC2P2	100/cCFA	2/3	2/18 (11%)	0.11±0.08
D	SC2P3	100/cCFA	3/3	7/18 (39%)	0.42±0.13
E	SC2P4	100/cCFA	1/3	2/18 (11%)	0.11±0.08
F	SC2P5	100/cCFA	1/3	1/18 (6%)	0.06±0.06
G	SC2P6	100/cCFA	3/3	3/18 (17%)	0.17±0.09
H	SC2P7	100/cCFA	1/3	1/18 (6%)	0.06±0.06
I	SC2P8	100/cCFA	2/3	3/18 (17%)	0.17±0.09
J	SC2P9	100/cCFA	3/3	4/18 (22%)	0.22±0.10
K	SC2P10	100/cCFA	2/2	4/12 (33%)	0.25±0.12
L	SC2P11	100/cCFA	3/3	5/18 (28%)	0.19±0.08
M	SC2P12	100/cCFA	1/2	2/12 (17%)	0.13±0.09
N	PBS	PBS/cCFA	2/3	2/18 (11%)	0.11±0.08

[a] Lewis rats were immunized with the indicated C-protein peptide in CFA along with pertussis toxin and sacrificed one week after the last immunization. Three rats per each peptide except for SC2P11 were immunized and examined histologically. The results for SC2 (Group A) and controls (Group N) listed in Table 2 are shown again for comparison.

[b] When inflammation was found in at least one site on hematoxylin and eosin-stained sections, rats were scored as positive.

[c] No. of muscle blocks containing inflammatory foci/No. of total blocks examined.

[d] Total histological scores/No. of blocks examined±SE.

[e] cCFA, conventional CFA containing 1 mg/ml *M. tuberculosis*.

[f] Significant differences were noted between the following two groups; A vs. J ($p<0.01$) and D vs. J ($p<0.05$).

were relatively spared (Fig. 2B, arrowheads). Since homology between fast-type and slow-type C-protein at the amino acid level is low (49.5% based on the NCBI database), it is possible that T cells activated by immunization with fast-type C-protein recruited mainly to fast-type fibers and not to slow-type fibers. Immunohistochemical examination demonstrated that predominant populations of infiltrating cells were αβ T cells (Fig. 2C) and macrophages (Fig. 2D) and that the number of γδ T and NK cells was small (data not shown). CD4 staining showed that the number and distribution of CD4-positive cells are almost the same as those of macrophages (Fig. 2E) because the CD4 molecules are expressed on both T cells and macrophages in rats (Jefferies et al., 1985). The number of CD8-positive cells was relatively small and CD4:CD8 ratio was 2.5±0.2. However, many of the CD8-positive cells were found at the interface of inflammation and remaining muscle fibers (Fig. 2F) and some were infiltrating muscle fibers (arrows in Fig. 2F), suggesting the importance of this cell type in lesion formation. These immunopathological findings are essentially the same as those found in native C-protein-induced EAM and human PM, implying that recombinant C-protein-induced EAM can serve as a model for human PM.

3.3. T and B cell epitopes in SC2-induced EAM

In order to characterize T and B cell epitopes, we focused on SC2 for further analysis for two reasons. First, SC2 showed high myositogenicity as demonstrated in Table 2. In addition, SC2 was hydrophilic, while SC3, which also showed intermediate myositogenicity, was hydrophobic and almost insoluble in water. Therefore, SC2 was more suitable for in vitro studies than SC3. For further analysis, we also produced overlapping synthetic peptides covering the SC2 molecule (Fig. 1 and Table 3). To identify T cell epitope(s), we next examined the proliferative responses of lymph node T cells taken from SC2-immunized animals (Fig. 3A). To screen the candidate peptide(s), peptide mixtures designated as Mix 1, 2, 3, and 4 were prepared. The mixtures contained 1–3, 4–6, 7–9, and 10–12, respectively.

A pilot study suggested that Mixture 2 contains T cell epitope (s). As clearly shown in Fig. 3A, Mixture 2 and immunizing protein, SC2, induced strong responses of T cells from SC2-immunized rats, while Mixtures 1, 3, and 4 induced only marginal responses. In a parallel assay, it was demonstrated that SC2P5, but not SC2P4 or SC2P6, in Mix 2 was responsible for T cell proliferation (Fig. 3A). We repeated the assays three times and obtained essentially the same results. Thus, it was clearly

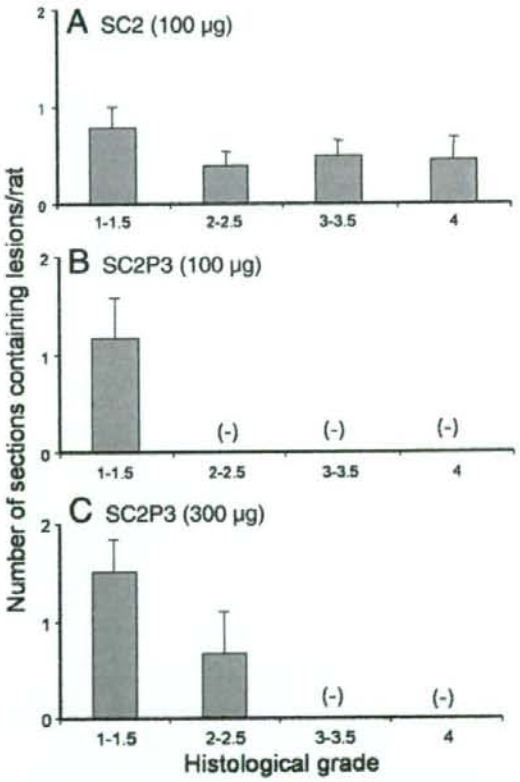

Fig. 4. Histological severities of muscle inflammation induced by immunization with SC2 (A), SC2P3 (100 μg) (B), and SC2P3 (300 μg) (C). The histological severities of EAM induced by three different immunogens were analyzed semiquantitatively. In SC2-induced EAM, rats developed almost equal proportions of Grade 1–4 lesions (A), whereas SC2P3-immunization induced only mild EAM (B). Increase of the immunogen resulted in the production of Grade 2–2.5 lesions, but not of Grade 3–4 lesions.

demonstrated that SC2P5 contains the T cell epitope. However, non-responder peptides could contain T cell epitope(s) because there is the possibility that long peptides used in the proliferation assay may not be properly processed and presented by APC.

Then, the B cell epitopes were determined using sera taken from SC2-immunized rats. As shown Fig. 3B, the level of anti-SC2 antibodies was elevated two weeks after the first immunization and reached a plateau thereafter. At four weeks after the first immunization, anti-SC2 antibodies reacted with SC2P3, and to lesser extent with SC2P7, in all the cases examined (Fig. 3C).

3.4. Identification of myositogenic epitopes in C-protein Fragment 2

Each peptide was immunized at a dose of 100 μg into rats and the results are summarized in Table 4. As clearly shown in Group D, SC2 Peptide 3 (SC2P3) exhibited the strongest myositogenicity in terms of the incidence (3/3), % inflammatory lesion (39%) and histological score (0.42±0.13) among 12 peptides tested. Immunization with other peptides induced no or marginal pathology compared with the PBS control. Although SC2P5 and SC2P7 contain T and B cell epitope, respectively, as shown in previous experiments, they did not show significant myositogenicity. Since SC2P3 induced mild EAM with this immunization protocol compared with SC2, we further tested its EAM-inducing ability with a stronger protocol. Immunization with SC2P3 at a higher dose (300 μg) emulsified in CFA containing *M. tuberculosis* at 5 mg/ml (5CFA) induced more severe EAM (1.03±0.32) with a higher frequency of inflammatory lesions (72%). However, there was still clear difference in histopathology between SC2P3- and SC2-induced EAM. Since we felt that in SC2P3-induced EAM, mild lesions were found more frequently than in SC2-induced EAM, we counted the number of lesions categorized in Scores of 1–1.5, 2–2.5, 3–

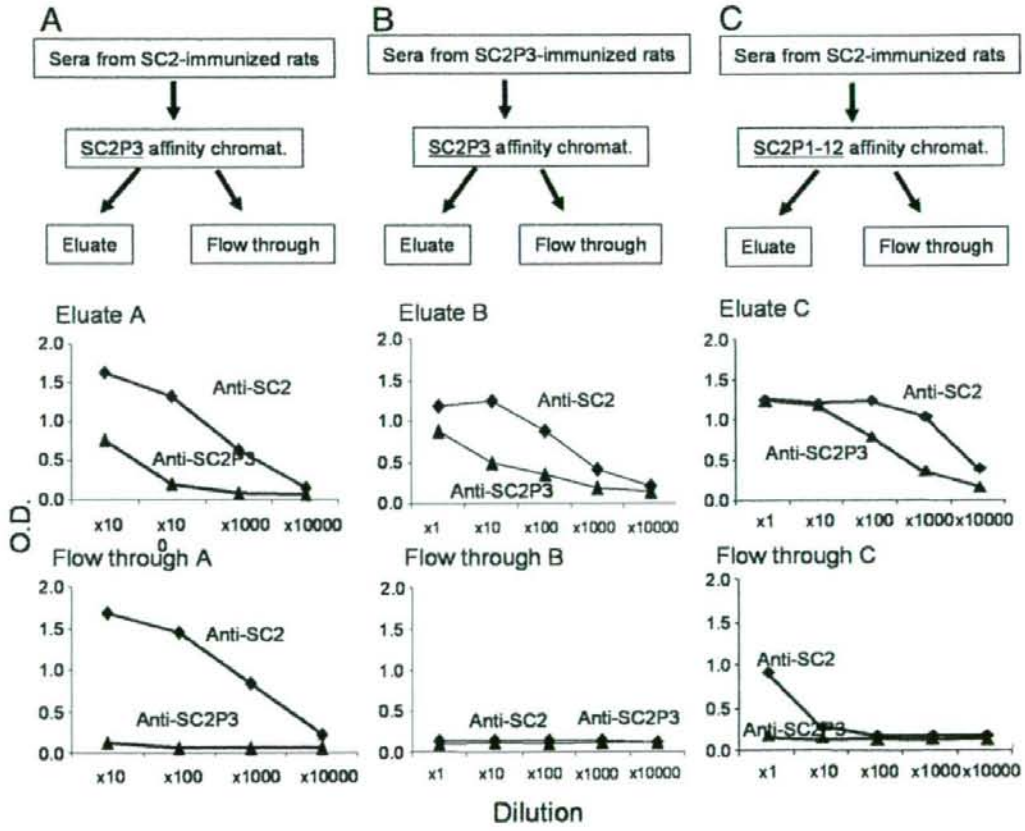

Fig. 5. Characterization of anti-SC2 and anti-SC2P3 antibodies in sera from SC2- or SC2P3-immunized rats using affinity chromatography. To characterize the nature of anti-SC2 and anti-SC2P3 antibodies in more detail, affinity columns coupled with either SC2P3 (A and B) or all the SC2 peptides (P1–P12) (C) were prepared and sera from SC2-immunized (A and C) or SC2P3-immunized (B) rats were passed through the columns. Then, the specificity of the eluate and flowthrough was analyzed by ELISA. When sera from SC2-immunized rats were applied to the SC2P3-coupled column, the eluate contained antibodies that reacted with SC2 and SC2P3 (Eluate A). In contrast, there were anti-SC2, but not anti-SC2P3, antibodies in the flowthrough fraction (Flow through A). Sera from SC2P3-immunized rats were also applied on the SC2P3-coupled column. In this case, all the anti-SC2 and anti-SC2P3 antibodies were captured on the column (Eluate B vs. Flow through B). Characteristically, sera from SC2-immunized rats contained antibodies that reacted with non-linear epitopes (Flow through C).

3.5 or 4 in each group. As clearly demonstrated in Fig. 4, SC2 induced inflammatory lesions with Scores 3–3.5 and 4 (Fig. 4A), whereas SC2P3 induced only mild lesions with Score 1–1.5 (Fig. 4B). Severe lesions with Score 2–2.5, 3–3.5, or 4 were not found in the latter group. Immunization with a higher dose of SC2P3 (300 μg) resulted in the formation of intermediately severe lesions with Score 2–2.5, but not of lesions with Score 3–3.5, or 4 (Fig. 4C). These findings strongly suggest that although SC2P3 contains major myositogenic epitope(s), it lacks factors that aggravate inflammatory lesions as found in SC2-induced EAM.

3.5. Characterization of autoantibodies generated after immunization with SC2 or SC2P3

The above findings raised the possibility that anti-SC2 antisera contain highly pathogenic antibodies that were absent in the SC2P3 antiserum preparation. To characterize the nature f the anti-SC2 antibodies in more detail, we prepared affinity columns coupled with either SC2P3 or all the SC2 peptides (P1–P12). Then, sera from SC2- or SC2P3-immunized rats were passed through the columns and the specificity of the eluate and flowthrough was analyzed by ELISA. The results are illustrated in Fig. 5. When sera from SC2-immunized rats were applied to the SC2P3-coupled column, the eluate contained antibodies that reacted with SC2 and SC2P3 (Eluate A of Fig. 5A). In contrast, there were anti-SC2, but not anti-SC2P3, antibodies in the flowthrough fraction (Flow through A of Fig. 5A). Similarly, sera from SC2P3-immunized rats were applied to the SC2P3-coupled column. In this case, all the anti-SC2 and anti-SC2P3 antibodies were captured on the column (Eluate B vs. Flow through B in Fig. 5B). Furthermore, Flow through C of anti-SC2 antisera that had been passed through the SC2P1-12 column contained anti-SC2 antibodies (Fig. 5C). These findings imply that anti-SC2 antisera contain anti-SC2 antibodies, possibly against the conformational epitope of the SC2 molecule, that do not bind with any of the SC2 peptides. In contrast, anti-SC2P3 antisera contained antibodies only reacting with SC2P3 (see Flow through B of Fig. 5B).

Table 5
SC2 peptide immunization plus antibody transfer experiments in EAM[a]

Group	Immunization	Ab transfer		Inflammation	
		Ab	Dose	Incidence	Score
A	SC2P5	Anti-SC2 sera	×5 dil (1 ml) × 2/w×3	3/3	0.28±0.09
B	SC2P5	SC2P mAb mix	2 mg×2/w×3	3/3	0.28±0.11
C	SC2P5	SC2P3.1 mAb (IgG1)	1 mg×2/w×3	3/3	0.28±0.11
D	SC2P5	SC2.1 mAb (IgG1)	1 mg×2/w×3	3/3	0.22±0.10
E	SC2P3	SC2.16 mAb (IgG2a)	1 mg×2/w×3	3/3	0.92±0.46
F	SC2P3	Saline	×2/w×3	3/3	0.67±0.46

[a] SC2P5 or SC2P3 peptide was immunized and the indicated sera (1 ml after 5-fold dilution) or mAb were injected intravenously twice a week for 3 weeks. Rats were examined histologically 2 weeks after the last antibody administration.

3.6. SC2 peptide immunization with co-transfer of anti-SC2 antibodies

Finally, we have tried to reproduce severe EAM compatible with SC2-induced EAM by SC2 peptide immunization plus co-transfer of polyclonal or monoclonal anti-SC2 antibodies (Table 5). Immunization with SC2P5 that contains the T cell epitope plus transfer of various types of anti-SC2 antibodies did not augment the severity of EAM (Groups A–D) compared with SC2P5 immunization alone (Table 4, Group F). SC2P3 immunization plus antibody transfer induced more severe EAM than SC2P3 immunization plus saline but there was no significant difference between the two groups (Group E vs. Group F). Thus, co-administration of anti-SC2 antibodies resulted in slight aggravation of peptide-induced AM but could not reproduce SC2-induced EAM.

4. Discussion

Polymyositis and dermatomyositis are muscle diseases characterized by the presence of muscle weakness and inflammatory infiltrates in the skeletal muscles (Dalakas, 1991). Although autoimmune processes are thought to be involved in the disease progression, these processes remain poorly understood. This is partly because there has been no good animal model for the detailed analysis. In a previous study (Kohyama and Matsumoto, 1999), we found that purified C-protein, a myosin-binding protein that comprises only 2% of the muscle components, possesses strong myositogenicity comparable with crude myosin and that its activity is much stronger than that of purified myosin. However, purified native C-protein has several limitations for detailed analysis. C-protein is a minor component of muscle proteins and therefore it is difficult to obtain a large amount of the protein (Offer, 1972; Offer et al., 1973). In addition, the purity and myositogenicity of the protein varied greatly from lot to lot, resulting in variation in the induction of EAM. In the present study, we characterized the role of pathogenic T and B cells in EAM hat had been induced by immunization with recombinant skeletal C-protein. Consequently, we obtained the following findings. First, all of the four recombinant C-protein fragments possessed myositis-inducing ability, indicating that the C-protein molecule contains multiple myositogenic epitopes. Second, in Fragment 2 of skeletal C-protein (SC2), which constantly induced severe EAM in Lewis rats, major T and B cell epitopes reside in SC2P5 (residues 84–412) and SC2P3 (residues 334–363), respectively. However, immunization with SC2P3, induced EAM but SC2P5 did not. Such discrepancy between the T and B cell epitopes was already observed in another autoimmune disease model. In experimental autoimmune encephalomyelitis (EAE) induced in Lewis rats by immunization with myelin basic protein MBP), the immunodominant epitope for encephalitogenic T cells resides within the 68–88 residues throughout the course of EAE (Vandenbark et al., 1985). In contrast, anti-MBP antibodies in the same strain react mainly with the 11–30 and 91–110 residues (Figueiredo et al., 1999).

It has been frequently reported that both autoreactive T cells and autoantibodies are involved in the pathogenesis of human PM. Clonal expansions of T cells, especially those bearing the CD8 phenotype, were observed in the peripheral blood of PM patients (Nishio et al., 2001; van der Meulen et al., 2002) and $CD8^+$ T cells with a similar characteristic infiltrated the muscle lesions (Arahata and Engel, 1984). In the present experiments, we demonstrated that T cells from SC2-immunized rats reacted only with SC2P5 but that SC2P5 immunization did not elicit EAM. These results suggest that simultaneous activation of pathogenic T and B cells is essential for the development of full-blown EAM.

With regard to autoantibodies in PM, there have been a number of reports demonstrating the presence of myositis-specific autoantibodies (MSA) (Brouwer et al., 2001; Mimori, 1999). For instance, anti-Jo-1 antibodies that recognize histidyl-tRNA synthetase are found in 20–30% of PM/DM patients. However, the role of MSA in the pathogenesis of PM remains almost unknown. Walker and Jeffrey speculated that through molecular mimicry among virus particles, Jo-1 antigen and muscle components such as myosin, autoantibodies raised after viral infection may attack Jo-1 antigen and the muscle (Walker and Jeffrey, 1986). Although it is possible, there is no direct evidence supporting this hypothesis. Curiously, there are no reports examining the presence or absence of autoantibodies against muscle components. As shown in the present study, autoantibodies against muscle components such as C-protein play a critical role in the development and progression of inflammatory myopathies. In sharp contrast to this situation, it was already demonstrated that anti-myocardial autoantibodies are present in patients with myocarditis and dilated cardiomyopathy (DCM) (Baba et al., 2001; Caforio et al., 2001, 2002) and removal of such antibodies by immunoadosorption induced early hemodynamic improvement (Felix et al., 2002).

On the basis of the findings obtained in T cell and autoantibody analysis, we tried to induce EAM comparable with SC2-induced EAM by SC2 peptide immunization plus adoptive transfer of various types of anti-SC2 antibodies, either polyclonal or monoclonal. Although co-transfer of anti-SC2 antibodies augmented the severity of SC2 peptide-induced EAM, we failed to induce full-blown EAM by this procedure. Furthermore, we have tried to induce passive EAM by adoptive transfer of SC2- or SC2 peptide-reactive T cells but failed to induce the disease. At least, two possibilities should be considered. First, it is possible that our protocol for antibody administration did not maintain sufficient antibody levels for lesion formation. The second possibility is that the barrier at the interface between the blood vessels and skeletal muscle (Dow et al., 1980) is so tight that the antibodies cannot enter muscle fibers even with the help of activated T cells. In this regard, it is interesting to note the results obtained in experimental autoimmune carditis (EAC). We already reported that EAC is inducible by immunization with cardiac C-protein fragment 2 (CC2) (Matsumoto et al., 2004) and observed B cell epitope spreading in rats that had been immunized with CC2, but not with CC2 peptide. In this case, peptide immunization plus anti-CC2 antibodies aggravated EAC (Matsumoto et al., 2007). Of course, these two possibilities do not exclude each other.

In summary, we have successfully induced EAM by immunization of recombinant SC2, and determined the myositogenic sequence in the SC2 molecule and the T and B cell epitopes. The data obtained in the present study provide useful information to analyze the pathomechanisms of the disease and to develop specific immunotherapies for PM in the near future.

Acknowledgements

This study was supported in part by Health and Labour Sciences Research Grants for Research on Psychiatric and Neurological Diseases and Mental Health and by Grants-in-Aid from the Japan Society for the Promotion of Science.

References

Arahata, K., Engel, A.G., 1984. Monoclonal antibody analysis of mononuclear cells in myopathies. I: Quantitation of subsets according to diagnosis and sites of accumulation and demonstration and counts of muscle fibers invaded by T cells. Ann. Neurol. 16, 193–208.

Baba, A., Yoshikawa, T., Chino, M., Murayama, A., Mitani, K., Nakagawa, S., Fujii, I., Shimada, M., Akaishi, M., Iwanaga, S., Asakura, Y., Fukuda, K., Mitamura, H., Ogawa, S., 2001. Characterization of anti-myocardial autoantibodies in Japanese patients with dilated cardiomyopathy. Jpn. Circ. J 65, 867–873.

Brouwer, R., Hengstman, G.J., Vree Egberts, W., Ehrfeld, H., Bozic, B., Ghirardello, A., Grondal, G., Hietarinta, M., Isenberg, D., Kalden, J.R., Lundberg, I., Moutsopoulos, H., Roux-Lombard, P., Vencovsky, J., Wikman, A., Seelig, H.P., van Engelen, B.G., van Venrooij, W.J., 2001. Autoantibody profiles in the sera of European patients with myositis. Ann. Rheum. Dis. 60, 116–123.

Caforio, A.L., Mahon, N.J., McKenna, W.J., 2001. Cardiac autoantibodies to myosin and other heart-specific autoantigens in myocarditis and dilated cardiomyopathy. Autoimmunity 34, 199–204.

Caforio, A.L., Mahon, N.J., Tona, F., McKenna, W.J., 2002. Circulating cardiac autoantibodies in dilated cardiomyopathy and myocarditis: pathogenetic and clinical significance. Eur. J. Heart Fail. 4, 411–417.

Dalakas, M.C., 1991. Polymyositis, dermatomyositis, and inclusion-body myositis. New Engl. J. Med. 325, 1487–1498.

Dalakas, M.C., 1992. Inflammatory Myopathy. Handbook of Clinical Neurology, Vol. 18(61). Elsevier, Amsterdam, pp. 369–390.

Dennis, J.E., Shimizu, T., Reinach, F.C., Fischman, D.A., 1984. Localization of C-protein isoforms in chicken skeletal muscle: ultrastructural detection using monoclonal antibodies. J. Cell Biol. 98, 1514–1522.

Dow, P.R., Shinn, S.L., Ovale Jr., W.K., 1980. Ultrastructural study of a blood-muscle spindle barrier after systemic administration of horseradish peroxidase. Am. J. Anat. 157, 375–388.

Engel, A.G., Arahata, K., 1984. Monoclonal antibody analysis of mononuclear cells in myopathies. II: Phenotypes of autoinvasive cells in polymyositis and inclusion body myositis. Ann. Neurol. 16, 209–215.

Felix, S.B., Staudt, A., Landsberger, M., Grosse, Y., Stangl, V., Spielhagen, T., Wallukat, G., Wernecke, K.D., Baumann, G., Stangl, K., 2002. Removal of cardiodepressant antibodies in dilated cardiomyopathy by immunoadsorption. J. Am. Coll. Cardiol. 39, 646–652.

Figueiredo, A.C., Cohen, I.R., Mor, F., 1999. Diversity of the B cell repertoire to myelin basic protein in rat strains susceptible and resistant to EAE. J. Autoimmun. 12, 13–25.

Fischman, D.A., Vaughan, K., Weber, F., Einheber, S., 1991. Myosin Binding Proteins: Intracellular Members of the Immunoglobulin Superfamily. Frontiers in muscle research, pp. 211–222.

Jefferies, W.A., Green, J.R., Williams, A.F., 1985. Authentic T helper CD4 (W3/25) antigen on rat peritoneal macrophages. J. Exp. Med. 162, 117–127.

Kohyama, K., Matsumoto, Y., 1999. C-protein in the skeletal muscle induces severe autoimmune polymyositis in Lewis rats. J. Neuroimmunol. 98, 130–135.

BRAIN RESEARCH 1162 (2007) 113–120

available at www.sciencedirect.com

ScienceDirect

www.elsevier.com/locate/brainres

BRAIN RESEARCH

Research Report

Increased phosphorylation of cyclic AMP response element-binding protein in the spinal cord of Lewis rats with experimental autoimmune encephalomyelitis

Heechul Kim[a,1], *Changjong Moon*[b,1], *Meejung Ahn*[a], *Yongduk Lee*[a], *Seungjoon Kim*[a], *Yoh Matsumoto*[c], *Chang-Sung Koh*[d], *Moon-Doo Kim*[e], *Taekyun Shin*[a,*]

[a]*Department of Veterinary Medicine and Applied Radiological Science Research Institute, Cheju National University, Jeju 690-756, South Korea*
[b]*Department of Veterinary Anatomy, College of Veterinary Medicine, Chonnam National University, Gwangju 500-757, South Korea*
[c]*Department of Molecular Neuropathology, Tokyo Metropolitan Institute for Neuroscience, Fuchu, Tokyo 183, Japan*
[d]*Department of Biomedical Laboratory Sciences, Shinshu University School of Health Sciences, 3-1-1 Asahi, Matsumoto 390-8621, Japan*
[e]*Department of Psychiatry, Cheju National University College of Medicine, Jeju 690-756, South Korea*

ARTICLE INFO

Article history:
Accepted 31 May 2007
Available online 21 June 2007

Keywords:
Astrocyte
Cyclic AMP response element-binding protein (CREB)
Experimental autoimmune encephalomyelitis (EAE)
Macrophage
Neuron

ABSTRACT

To investigate whether the phosphorylation of cyclic AMP response element-binding protein (CREB) is implicated in the pathogenesis of experimental autoimmune encephalomyelitis (EAE), the change in the level of CREB phosphorylation was analyzed in the spinal cord of Lewis rats with EAE. Western blot analysis showed that the phosphorylation of CREB in the spinal cord of rats increased significantly at the peak stage of EAE compared with the controls ($p<0.05$) and declined significantly in the recovery stage ($p<0.05$). Immunohistochemistry showed that the phosphorylated form of CREB (p-CREB) was constitutively immunostained in few astrocytes and dorsal horn neurons in the spinal cord of normal rats. In the EAE-affected spinal cord, p-CREB was mainly found in ED1-positive macrophages at the peak stage of EAE, and the number of p-CREB-immunopositive astrocytes was markedly increased in the spinal cord with EAE compared with the controls. Moreover, p-CREB immunoreactivity of sensory neurons, which are closely associated with neuropathic pain, was significantly increased in the dorsal horns at the peak stage of EAE. Based on these results, we suggest that the increased phosphorylation of CREB in EAE lesions was mainly attributable to the infiltration of inflammatory cells and astrogliosis, possibly activating gene transcription, and that its increase in the sensory neurons in the dorsal horns is involved in the generation of neuropathic pain in the rat EAE model.

* *Corresponding author.* Fax: +82 64 756 3354.
E-mail address: shint@cheju.ac.kr (T. Shin).
[1] The first two authors contributed to this work equally.

0006-8993/$ – see front matter © 2007 Elsevier B.V. All rights reserved.
doi:10.1016/j.brainres.2007.05.072

1. Introduction

Cyclic AMP response element-binding protein (CREB) is a transcription factor (Brindle and Montminy, 1992) that was originally shown to be phosphorylated at serine residue 133 (Ser-133) by an activated cAMP-dependent protein kinase A and mitogen activated protein kinases (MAPKs). The phosphorylation of this residue allows the recruitment of CREB-binding protein (CBP) or its paralogue, p300 (Johannessen et al., 2004; Roach et al., 2005). CREB regulates responses to growth factors, inflammatory mediators, and some cell-activating agents by binding to cAMP response elements (CRE) (Caivano and Cohen, 2000; Liu et al., 2004; Ma and Eisenach, 2002; Mayr and Montminy, 2001). The phosphorylation of CREB participates in a wide range of cellular events in the nervous system, including neuronal differentiation (Bender et al., 2001), neuronal survival (Ryu et al., 2005), neuropathic pain (Ma and Quirion, 2001), and inflammation (Etienne-Manneville et al., 1999). Little is known about the phosphorylation of CREB in autoimmune central nervous system (CNS) disease models such as experimental autoimmune encephalomyelitis (EAE), which is characterized by reactive gliosis as well as infiltration of autoimmune T and bystander cells (Schonrock et al., 1998; Shin et al., 1995, 2003).

Our previous studies have shown that the MAPK pathway, which is upstream of CREB, is activated in autoimmune inflammation in the nervous system (Ahn et al., 2004; Moon et al., 2005; Shin et al., 2003) and that the resulting pro-inflammatory cytokines are associated with the induction of EAE paralysis (Tanuma et al., 1997). These factors are associated with the activation of CREB in each cell type.

The aim of the present study was to determine whether CREB is implicated in the course of EAE, which is an animal model of human multiple sclerosis.

2. Results

2.1. *Clinical progression of experimental autoimmune encephalomyelitis and histopathological findings*

EAE-affected rats immunized with myelin basic protein (MBP) developed floppy tails (grade 1, G.1) on days 9–11 post-immunization (p.i.) and exhibited progressive hind limb paralysis (G.2 or G.3) on days 12–14 p.i. All of the rats recovered on day 21 p.i. (recovery 0, R.0).

Histopathological examination showed no infiltrating cells in the spinal cord of the normal controls (Fig. 1A). With hind limb paralysis, inflammatory cells infiltrated the parenchyma of the spinal cord in EAE-affected rats (day 12 p.i.; Fig. 1B). In the EAE lesions, most of the inflammatory cells were ED1-positive macrophages (Fig. 1C) and monoclonal anti-T cell receptor αβ (R73)-positive T cells (Fig. 1D). The clinical observations and histological findings related to EAE largely corresponded to those described previously (Shin et al., 1995, 2003).

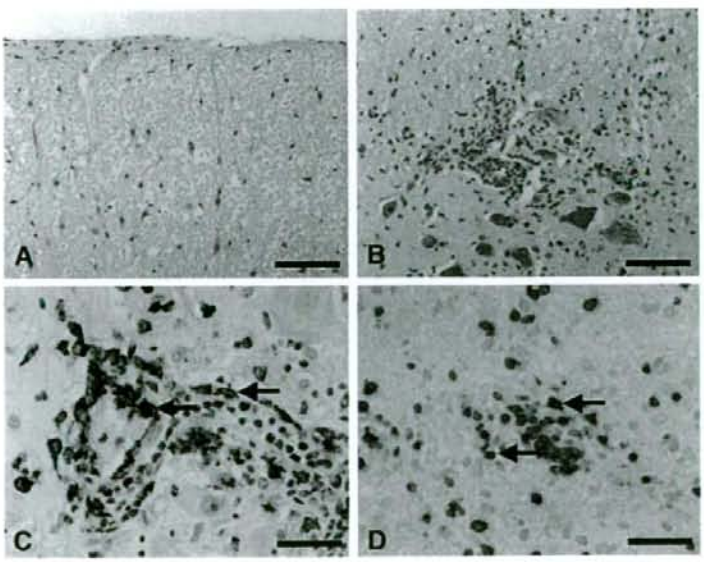

Fig. 1 – Histopathological examination of normal and EAE-affected rat spinal cords. (A) There are no inflammatory cells in the spinal cords of the normal control rats. (B) On day 12 after the injection of myelin basic protein, many inflammatory cells are present in the spinal cord of EAE-affected rats. (C, D) The majority of the inflammatory cells within the EAE lesions are ED1-positive macrophages (C, arrows) and R73 (TCR αβ)-positive T cells (D, arrows). A and B: hematoxylin–eosin staining. C and D: immunostained with either ED1 (C) or R73 (D) and counterstained with hematoxylin. Scale bars: in panels A and B, 80 μm; in panels C and D, 40 μm.

2.2. *Activation of CREB and ATF-1 in the spinal cord in EAE*

Antibody to the phosphorylated form of CREB (p-CREB) detects endogenous levels of CREB only when CREB is phosphorylated at Ser-133 and also detects the phosphorylated form of CREB-related protein activating transcription factor-1 (p-ATF-1). Therefore, we used different normalized bands for the analysis of p-CREB and p-ATF-1; the intensity of p-CREB was normalized to CREB, and the intensity of p-ATF-1 was normalized to beta-actin.

The level of p-CREB in the spinal cord was semiquantitatively evaluated during the course of EAE, using Western blot analysis. The expression of p-CREB immunoreactivity was detected at low levels in the spinal cord of normal control rats (density, 0.35 ± 0.06 OD/mm^2; $n=5$); it significantly increased in the spinal cord during the peak stage of EAE (G.3, day 12 p.i.; 1.57 ± 0.15 OD/mm^2; $n=5$; $p<0.05$ vs. controls) and subsequently declined in the recovery stage (R.0, day 21 p.i.; 0.34 ± 0.07 OD/mm^2; $n=5$; $p<0.05$ vs. peak stage of EAE) (Fig. 2).

The expression of p-ATF-1 immunoreactivity was also detected at low levels in the spinal cord of normal control rats (0.26 ± 0.04 OD/mm^2; $n=5$); it significantly increased in the spinal cord in the peak stage of EAE (G.3, day 12 p.i.; 0.84 ± 0.13 OD/mm^2; $n=5$; $p<0.05$ vs. controls). The expression was slightly lower in the recovery stage of EAE (R.0, day 21 p.i.; 0.53 ± 0.1 OD/mm^2; $n=5$) but was still higher than the control level ($p<0.05$ vs. controls) (Fig. 2).

2.3. *Localization of p-CREB in spinal cord sections from EAE-affected rats*

2.3.1. *p-CREB immunoreactivity*

Immunohistochemically, p-CREB was detected in a few glial cells in the normal rat spinal cord (Fig. 3A). In the peak stage of EAE (G.3, day 12 p.i.), many p-CREB-positive glial cells were detected in the white (Fig. 3B) and gray (data not shown) matter of the spinal cord. In addition, during the peak stage of EAE, there was massive infiltration of inflammatory cells in the parenchyma, where some round cells were positive for p-CREB (Fig. 3C). In the recovery stage of EAE (R.0, day 21 p.i.), there were fewer inflammatory cells than in the peak stage, and a few glial cells were positive for p-CREB (Fig. 3D).

In addition, p-CREB was detected in neurons in the dorsal horn lamina of the normal rat spinal cord (mean number± SEM: 39.57±7.62) (Fig. 4A). In the peak stage of EAE (G.3, day 12 p.i.), p-CREB-positive neurons in the dorsal horn lamina were increased compared with normal control rats (66.57±7.62; $p<0.05$ vs. controls) (Fig. 4B); the immunoreactivity decreased

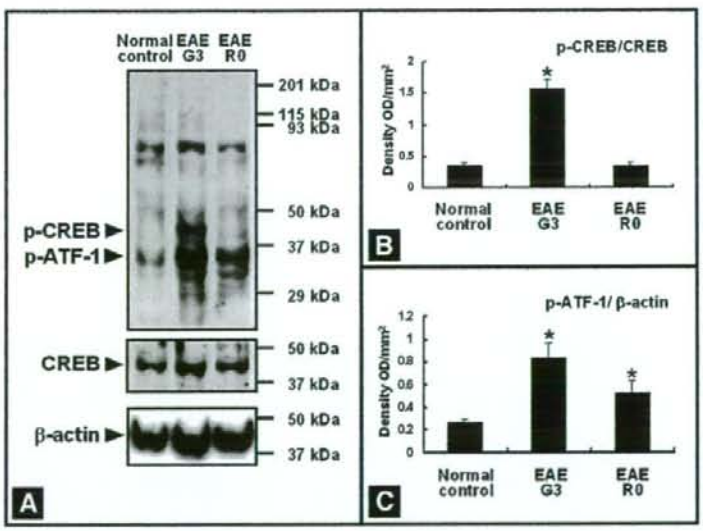

Fig. 2 – Western blot analysis of p-CREB and p-ATF-1 expression in the spinal cord of rats with EAE. Spinal cord samples were collected from normal control rats, rats at the peak stage of EAE (day 12 p.i.; stage G.3), and rats during the recovery stage (day 21 p.i.; stage R.0). (A) Representative photographs of Western blots; arrowheads indicate the expression of p-CREB (~43 kDa), p-ATF-1 (~35 kDa), CREB (~43 kDa), and beta-actin (~45 kDa). (B) Semiquantitative analysis of p-CREB immunoreactivity in spinal cords, normalized to the intensity of CREB expression in the same immunoblot. The p-CREB expression is significantly greater in spinal cords from rats sacrificed at the peak of EAE (G.3, $p<0.05$) than in spinal cords from control rats, and the expression level declines to control levels during the recovery stage (R.0) from EAE. Data (mean ± SEM) are from five experiments. *$p<0.05$ vs. normal controls and the recovery stage of EAE. (C) Semiquantitative analysis of p-ATF-1 immunoreactivity in spinal cords, normalized to the intensity of beta-actin expression in the same immunoblot. p-ATF-1 is detected in the normal controls, and its expression is significantly increased in EAE-affected spinal cords. *$p<0.05$ vs. normal controls.

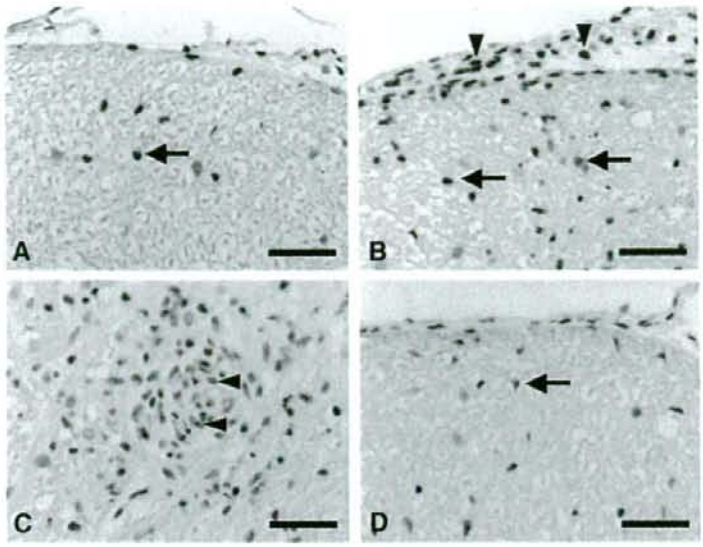

Fig. 3 – Immunohistochemical staining of p-CREB in the spinal cords of normal control rats (A) and rats at the peak (day 12 p.i.) (B, C) and recovery stages of EAE (day 21 p.i.) (D). (A) p-CREB is weakly detected in some glial cells (arrow) in the spinal cord of normal control rats. (B, C) In the peak stage of EAE, glial cells show increased immunoreactivity for p-CREB (B, arrows), and p-CREB-positive inflammatory cells are detected in the subarachnoid space (B, arrowheads) and parenchyma (C, arrowheads). (D) In the recovery stage of EAE, some p-CREB immunoreactive cells remain (arrow). Counterstained with hematoxylin. Scale bars: 40 μm.

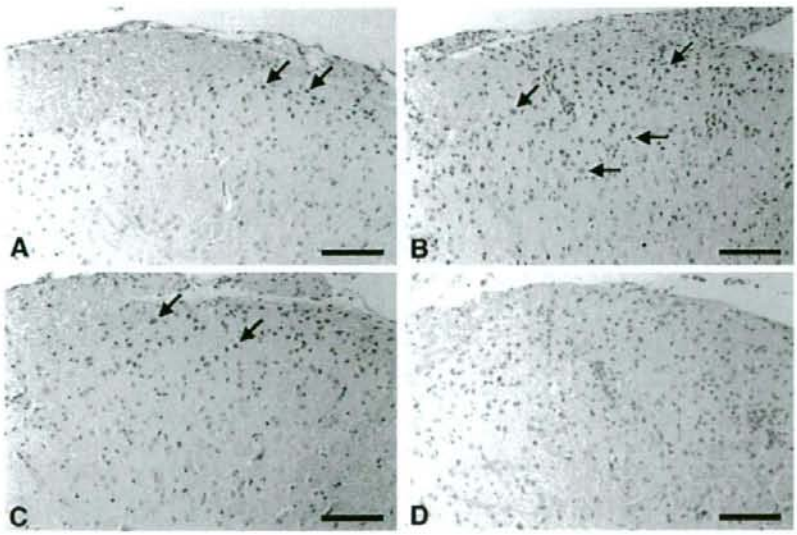

Fig. 4 – Immunohistochemical staining of p-CREB in the dorsal horn lamina in the spinal cords of normal control rats (A) and rats at the peak (day 12 p.i.) (B) and recovery stages of EAE (day 21 p.i.) (C). (A) p-CREB is constitutively immunostained in the dorsal horn lamina in the normal controls. (B, C) The p-CREB immunoreactivity is significantly increased in the dorsal horn lamina in the peak stage (B) and has declined in the recovery stage of EAE (C). (D) Tissue from a rat in the peak stage of EAE stained without primary antisera shows no staining. Counterstained with hematoxylin. Scale bars: 100 μm.

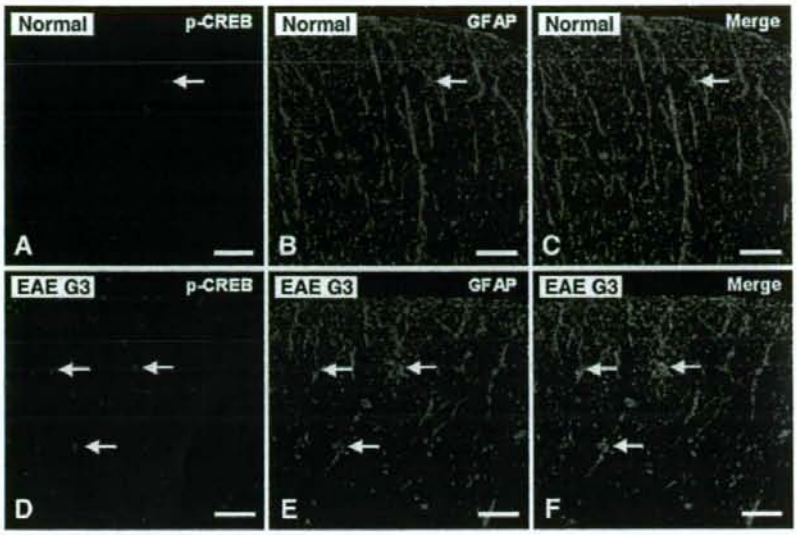

Fig. 5 – Immunofluorescent co-localization of p-CREB (A, D; red) with anti-GFAP (B, E; green) in the spinal cords of normal control rats (A–C) and rats at the peak stage of EAE (day 12 p.i.) (D–F). (A–C) In the normal controls, some p-CREB-immunopositive glial cells are co-localized in GFAP-positive astrocytes in the spinal cords (arrows). (D–F) In the EAE-affected spinal cords, many p-CREB-positive glial cells were positive for GFAP (arrows). C and F are merged images. Scale bars: 50 μm.

significantly in the recovery stage of EAE (43.86±5.2; $p<0.05$ vs. peak stage of EAE) (Fig. 4C). Some p-CREB-positive ependymal cells were detected in the spinal cords of normal control rats and rats with EAE (data not shown).

2.3.2. Identification of p-CREB-positive cells in the spinal cords of normal controls and rats with EAE

The patterns of p-CREB immunofluorescence in the spinal cords of normal control rats and rats with EAE were similar to those seen with single immunoperoxidase staining (Figs. 3 and 4). Very little p-CREB (Fig. 5A, red) was immunodetected in GFAP-positive-astrocytes (Fig. 5B, green) in the control spinal cord (Fig. 5C, merge). In the EAE spinal cord (day 12 p.i.), p-CREB-positive astrocytes increased (Figs. 5D–F). p-CREB (Fig. 6A, red) was abundant in ED1-positive cells (Fig. 6B, green; Fig. 6C, merge), suggesting that the majority of macrophages were positive for p-CREB in EAE lesions at the peak stage.

3. Discussion

This study is the first to show that a gene transcription factor, CREB, is phosphorylated in host and inflammatory cells in the spinal cord of animals with EAE, particularly during the peak stage, suggesting that CREB phosphorylation is closely associated with autoimmune inflammatory attack in the spinal cord.

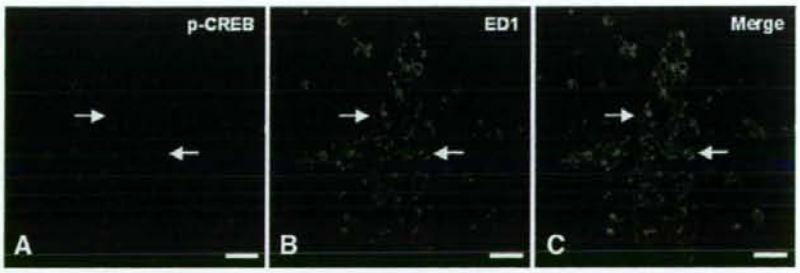

Fig. 6 – Immunofluorescent co-localization of p-CREB (A) with ED1 (B) in the spinal cord of rats in the peak stage of EAE (day 12 p.i.). A large amount of p-CREB (A, red; arrows) was immunostained in ED1-positive macrophages (B, green; arrows) (C, merge; arrows). Scale bars: in A–C, 20 μm.

With regard to the phosphorylation of CREB in the peak stage of EAE, the activation of CREB has been associated with signal enzymes such as MAPKs (Shin et al., 2003) as well as pro-inflammatory cytokines, including interferon-γ (IFN-γ) and tumor necrosis factor-α (TNF-α) (Renno et al., 1995; Tanuma et al., 1997). The MAPKs transduce a variety of extracellular stimuli through a cascade of protein phosphorylation, leading to the activation of gene transcription factors (Seger and Krebs, 1997). Two potential *in vivo* substrates for the MAPK pathway are CREB and the closely related ATF-1. MAPKs phosphorylate CREB at Ser-133 (Johannessen et al., 2004). Moreover, several further lines of evidence are consistent with the hypothesis that CREB and ATF-1 become phosphorylated at the relevant sites in response to growth factors, inflammatory mediators, and some cell-activating and -damaging stimuli (Caivano and Cohen, 2000; Kingsley-Kallesen et al., 1999; Zaman et al., 1999). This study confirms that the phosphorylation of CREB in EAE lesions occurs in the inflammatory cells, astrocytes, and neurons, which corresponds to the increased phosphorylation of MAPKs in rats with EAE as reported in our previous study (Shin et al., 2003). Thus, we postulate that the activation of MAPKs affects the phosphorylation of CREB in affected cells in the spinal cord with EAE through the activation of CREB and ATF-1 signaling pathways.

In response to stimuli, macrophages undergo a series of processes such as chemotaxis, phagocytosis, and the release of inflammatory mediators (Rotshenker, 2003). IFN-γ has been shown to activate the CREB signaling pathway in murine peritoneal macrophages (Liu et al., 2004), and the activation of CREB/ATF-1 promotes the production of pro-inflammatory cytokines such as TNF-α and interleukin-1β (IL-1β) in lipopolysaccharide (LPS)-stimulated macrophages (Caivano and Cohen, 2000). The inflammatory mediators (IFN-γ and TNF-α) described above have been closely associated with EAE lesions (Renno et al., 1995; Tanuma et al., 1997). Considering the data obtained from the present study, we postulate that pro-inflammatory cytokines, including IFN-γ, activate ED1-positive macrophages with an increased phosphorylation of CREB, possibly leading to the further production of pro-inflammatory cytokines, including TNF-α.

With regard to the inflammatory stimuli involved in the phosphorylation of CREB in astrocytes, which are an important cell type in EAE, it is known that LPS induces an increase in CREB phosphorylation via the MAPK pathway in cultured astrocytes (Buzas et al., 2002). In addition, LPS has been associated with the induction of IL-1 and TNF-α in cultured human astrocytes (Velasco et al., 1991). In the present study, we found that the phosphorylation of CREB increased in reactive astrocytes in the peak stage of EAE, suggesting that CREB activation may be involved in the gene transcription of inflammatory mediators in autoimmune-stimulated astrocytes as well as in macrophages.

Although the phosphorylation of CREB has been immunodetected at intense levels in macrophages and astrocytes in EAE, it was also found in the dorsal horn neurons in the peak stage of EAE in the present study. This finding implies that increased phosphorylation of CREB plays an important role in the sensory function during the course of EAE. There is a general consensus that the phosphorylation of CREB in dorsal horn neurons is possibly involved in the generation and maintenance of neuropathic pain caused by partial sciatic nerve ligation (Ma and Quirion, 2001) and spinal cord injury (Crown et al., 2006).

It was recently shown that, in both active and passive EAE, there was an initial increase in tail withdrawal latency (hypoalgesia) that peaked several days prior to the peak in motor deficits during the acute disease phase (Aicher et al., 2004). Considering these results, it is highly possible that increased CREB phosphorylation in the dorsal horn neurons in the spinal cord of rats with EAE leads to the generation and maintenance of neuropathic pain.

When all the findings are taken into consideration, they suggest that increased phosphorylation of CREB occurs in the spinal cord in the peak stage of EAE and contributes to the activation of inflammatory cells such as macrophages, to the occurrence of reactive astrogliosis, and partially to the generation of neuropathic pain during the course of rat EAE and possibly in human multiple sclerosis.

4. Experimental procedures

4.1. *Animals*

Lewis rats were obtained from Harlan (Indianapolis, IN) and were bred in our animal facility. Male rats (7–8 weeks old; 160–200 g) were used in this study. All experiments followed accepted ethical guidelines.

4.2. *Induction of experimental autoimmune encephalomyelitis*

The footpads of both hind feet of rats in the EAE group were injected with 100 μl of an emulsion that contained equal parts of MBP (1 mg/ml) and complete Freund's adjuvant (CFA) supplemented with *Mycobacterium tuberculosis* H37Ra (5 mg/ml) (Difco, Detroit, MI). Control rats were immunized with CFA only. After immunization, the rats were observed daily for clinical signs of EAE. The progression of EAE was divided into seven clinical stages: Grade 0 (G.0), no signs; G.1, floppy tail; G.2, mild paraparesis; G.3, severe paraparesis; G.4, tetraparesis; G.5, moribund condition or death; and R.0, recovery (Shin et al., 1995).

4.3. *Antibodies*

Rabbit polyclonal anti-p-CREB (Ser-133) and anti-CREB antibodies were obtained from Cell Signaling Technology (Beverly, MA). The p-CREB antibody also detects the phosphorylated form of CREB-related protein ATF-1 (as characterized by the manufacturer). Mouse monoclonal anti-beta-actin and mouse anti-GFAP were obtained from Sigma (St. Louis, MO). ED1 (mouse monoclonal anti-rat macrophages) was obtained from Serotec (London, UK). R73 (mouse monoclonal anti-T cell receptor αβ) was obtained from Blackthorn (Bicester, Bucks, UK).

4.4. *Tissue sampling*

The rats were sacrificed under ether anesthesia. The spinal cords were dissected from each group at 12–14 and 21 days p.i.

(n=5 rats/group); these periods coincided with the peak (G.3, day 12–14 p.i.) and recovery (R.0, day 21 p.i.) stages of EAE. Samples of the spinal cords were processed for embedding in paraffin wax after fixation in 4% paraformaldehyde in phosphate-buffered saline (PBS, pH 7.4). Paraffin sections (5 μm thick) were used for all immunostaining, except for the T cell marker R73. For T cell immunostaining, pieces of the spinal cords were snap-frozen in optimal cutting temperature compound (Sakura, Tokyo, Japan), and sections (8 μm thick) were cut using a cryostat (Leica, Nussloch, Germany). Additional spinal cord samples were snap-frozen and stored for immunoblot analysis.

4.5. *Western blot analysis*

The spinal cord tissue was homogenized in modified radioimmunoprecipitation assay (RIPA) buffer (20 mM Tris, pH 7.5, 150 mM NaCl, 1% Triton-X 100, 0.5% sodium deoxycholate, 0.1% sodium dodecyl sulfate, 1% NP-40, 10 mM NaF, 1 mM EDTA, 1 mM EGTA, 1 mM Na_3VO_4, 1 mM PMSF, 10 μg/ml aprotinin, and 10 μg/ml leupeptin) with 20 strokes in a homogenizer. The homogenate was transferred to microtubes and centrifuged at 14,000 rpm for 20 min, and the supernatant was harvested.

For the immunoblot assay, supernatant samples containing 40 μg of protein each were loaded into individual lanes of 10% sodium dodecyl (lauryl) sulfate-polyacrylamide gels, electrophoresed, and immunoblotted onto nitrocellulose membranes (Schleicher and Schuell, Keene, NH). The residual binding sites on the membrane were blocked by incubation with 5% nonfat milk in Tris-buffered saline (TBS; 10 mM Tris–HCl, pH 7.4, and 150 mM NaCl) for 1 h. Subsequently, the membrane was incubated for 2 h with rabbit polyclonal anti-p-CREB (1:1000 dilution) antibody. The membranes were washed three times in TBS containing 0.1% Tween 20 and then incubated with horseradish peroxidase-conjugated anti-rabbit IgG (Vector, Burlingame, CA) for 1 h. Bound antibodies were detected using chemiluminescent substrate (WEST-one™ Kit; iNtRON Biotech Inc., Kyungki, Korea) according to the manufacturer's instructions. After imaging, the membranes were stripped and reprobed using anti-CREB and anti-beta-actin antibodies. The optical density (per mm^2) of each band was measured with a scanning laser densitometer (GS-700, Bio-Rad, Hercules, CA), and these values are presented as means± SEM. The ratios of the density of each p-CREB or p-ATF-1 band relative to that of the CREB or beta-actin band, respectively, were compared using Molecular Analyst software (Bio-Rad).

The data were analyzed using one-way ANOVA followed by the Student–Newman–Keuls *post hoc* test for multiple comparisons. In all cases, $p<0.05$ was taken as statistically significant.

4.6. *Immunohistochemistry*

Paraffin sections were used for the immunoperoxidase staining of p-CREB and rat macrophages, and frozen sections were used for the detection of T cells.

Briefly, paraffin-embedded spinal cords (5-μm sections) were deparaffinized by treatment with citrate buffer (0.01 M, pH 6.0) in a microwave for 10 min. To identify T cells, the frozen spinal cord sections were air-dried and fixed in 4% paraformaldehyde buffered with 0.1 M PBS (pH 7.2) for 20 min. After three washes with PBS, the sections were treated with 0.3% hydrogen peroxide in methyl alcohol for 20 min to block endogenous peroxidase activity.

After three washes with PBS, the sections were incubated with 10% normal goat or horse serum and then with the primary antigens, including rabbit polyclonal anti-p-CREB (1:200 dilution), ED1 (1:800 dilution), and R73 (1:1,000 dilution). Immunoreactivity was visualized using the avidin–biotin peroxidase reaction (Vector Elite kit, Vector, Burlingame, CA). Peroxidase was developed using a diaminobenzidine substrate kit (Vector). Sections were counterstained with hematoxylin before mounting. As a control, the primary antisera were omitted for a few test sections in each experiment.

To examine the cell phenotype in p-CREB expression, double immunofluorescence was applied using cell type-specific markers: ED1 for monocyte-like macrophages and anti-GFAP for astrocytes. First, paraffin sections were reacted sequentially with rabbit anti-p-CREB (1:100 dilution), biotinylated anti-rabbit IgG (Vector) (1:200 dilution), and tetramethyl rhodamine isothiocyanate (TRITC)-labeled streptavidin (Zymed, San Francisco, CA) (1:1,000 dilution). The slides were then incubated with ED1 (1:200 dilution) and anti-GFAP (1:200 dilution), followed by fluorescein isothiocyanate (FITC)-labeled goat anti-mouse IgG (1:50 dilution; Sigma).

To minimize lipofuscin autofluorescence, the sections were washed in PBS (3×1 h) at RT, dipped briefly in distilled H_2O, treated with 10 mM $CuSO_4$ in ammonium acetate buffer (50 mM CH_3COONH_4, pH 5.0) for 20 min, dipped briefly again in distilled H_2O, and then returned to PBS. The double immunofluorescence-stained specimens were examined under an FV500 laser confocal microscope (Olympus, Tokyo, Japan).

To semiquantify the immunostaining for p-CREB-positive neurons in the dorsal horn lamina, the number of p-CREB-positive dorsal horn neurons was counted in seven spinal cords from each group.

REFERENCES

Ahn, M., Moon, C., Lee, Y., Koh, C.S., Kohyama, K., Tanuma, N., Matsumoto, Y., Kim, H.M., Kim, S.R., Shin, T., 2004. Activation of extracellular signal-regulated kinases in the sciatic nerves of rats with experimental autoimmune neuritis. Neurosci. Lett. 372, 57–61.

Aicher, S.A., Silverman, M.B., Winkler, C.W., Bebo Jr., B.F., 2004. Hyperalgesia in an animal model of multiple sclerosis. Pain 110, 560–570.

Bender, R.A., Lauterborn, J.C., Gall, C.M., Cariaga, W., Baram, T.Z., 2001. Enhanced CREB phosphorylation in immature dentate gyrus granule cells precedes neurotrophin expression and indicates a specific role of CREB in granule cell differentiation. Eur. J. Neurosci. 13, 679–686.

Brindle, P.K., Montminy, M.R., 1992. The CREB family of transcription activators. Curr. Opin. Genet. Dev. 2, 199–204.

Buzas, B., Rosenberger, J., Kim, K.W., Cox, B.M., 2002. Inflammatory mediators increase the expression of nociceptin/orphanin FQ in rat astrocytes in culture. Glia 39, 237–246.

Caivano, M., Cohen, P., 2000. Role of mitogen-activated protein kinase cascades in mediating lipopolysaccharide-stimulated

induction of cyclooxygenase-2 and IL-1β in RAW264 macrophages. J. Immunol. 164, 3018–3025.

Crown, E.D., Ye, Z., Johnson, K.M., Xu, G.Y., McAdoo, D.J., Hulsebosch, C.E., 2006. Increases in the activated forms of ERK 1/2, p38 MAPK, and CREB are correlated with the expression of at-level mechanical allodynia following spinal cord injury. Exp. Neurol. 199, 397–407.

Etienne-Manneville, S., Chaverot, N., Strosberg, A.D., Couraud, P.O., 1999. ICAM-1-coupled signaling pathways in astrocytes converge to cyclic AMP response element-binding protein phosphorylation and TNF-alpha secretion. J. Immunol. 163, 668–674.

Johannessen, M., Delghandi, M.P., Moens, U., 2004. What turns CREB on? Cell Signal 16, 1211–1227.

Kingsley-Kallesen, M.L., Kelly, D., Rizzino, A., 1999. Transcriptional regulation of the transforming growth factor-beta2 promoter by cAMP-responsive element-binding protein (CREB) and activating transcription factor-1 (ATF-1) is modulated by protein kinases and the coactivators p300 and CREB-binding protein. J. Biol. Chem. 274, 34020–34028.

Liu, L., Wang, Y., Fan, Y., Li, C.L., Chang, Z.L., 2004. IFN-gamma activates cAMP/PKA/CREB signaling pathway in murine peritoneal macrophages. J. Interferon Cytokine Res. 24, 334–342.

Ma, W., Eisenach, J.C., 2002. Morphological and pharmacological evidence for the role of peripheral prostaglandins in the pathogenesis of neuropathic pain. Eur. J. Neurosci. 15, 1037–1047.

Ma, W., Quirion, R., 2001. Increased phosphorylation of cyclic AMP response element-binding protein (CREB) in the superficial dorsal horn neurons following partial sciatic nerve ligation. Pain 93, 295–301.

Mayr, B., Montminy, M., 2001. Transcriptional regulation by the phosphorylation-dependent factor CREB. Nat. Rev., Mol. Cell Biol. 2, 599–609.

Moon, C., Ahn, M., Kim, H., Lee, Y., Koh, C.S., Matsumoto, Y., Shin, T., 2005. Activation of p38 mitogen-activated protein kinase in the early and peak phases of autoimmune neuritis in rat sciatic nerves. Brain Res. 1040, 208–213.

Renno, T., Krakowski, M., Piccirillo, C., Lin, J.Y., Owens, T., 1995. TNF-alpha expression by resident microglia and infiltrating leukocytes in the central nervous system of mice with experimental allergic encephalomyelitis. Regulation by Th1 cytokines. J. Immunol. 154, 653–944.

Roach, S.K., Lee, S.B., Schorey, J.S., 2005. Differential activation of the transcription factor cyclic AMP response element binding protein (CREB) in macrophages following infection with pathogenic and nonpathogenic mycobacteria and role for CREB in tumor necrosis factor alpha production. Infect. Immun. 73, 514–522.

Rotshenker, S., 2003. Microglia and macrophage activation and the regulation of complement-receptor-3 (CR3/MAC-1)-mediated myelin phagocytosis in injury and disease. J. Mol. Neurosci. 21, 65–72.

Ryu, H., Lee, J., Impey, S., Ratan, R.R., Ferrante, R.J., 2005. Antioxidants modulate mitochondrial PKA and increase CREB binding to D-loop DNA of the mitochondrial genome in neurons. Proc. Natl. Acad. Sci. U. S. A. 102, 13915–13920.

Schonrock, L.M., Kuhlmann, T., Adler, S., Bitsch, A., Bruck, W., 1998. Identification of glial cell proliferation in early multiple sclerosis lesions. Neuropathol. Appl. Neurobiol. 24, 320–330.

Shin, T., Ahn, M., Jung, K., Heo, S., Kim, D., Jee, Y., Lim, Y.K., Yeo, E.J., 2003. Activation of mitogen-activated protein kinases in experimental autoimmune encephalomyelitis. J. Neuroimmunol. 140, 118–125.

Shin, T., Kojima, T., Tanuma, N., Ishihara, Y., Matsumoto, Y., 1995. The subarachnoid space as a site for precursor T cell proliferation and effector T cell selection in experimental autoimmune encephalomyelitis. J. Neuroimmunol. 56, 171–178.

Seger, R., Krebs, E.G., 1997. The MAPK signaling cascade. FASEB J. 9, 726–735.

Tanuma, N., Kojima, T., Shin, T., Aikawa, Y., Kohji, T., Ishihara, Y., Matsumoto, Y., 1997. Competitive PCR quantification of pro- and anti-inflammatory cytokine mRNA in the central nervous system during autoimmune encephalomyelitis. J. Neuroimmunol. 73, 197–206.

Velasco, S., Tarlow, M., Olsen, K., Shay, J.W., McCracken Jr., G.H., Nisen, P.D., 1991. Temperature-dependent modulation of lipopolysaccharide-induced interlukin-1 beta and tumor necrosis factor alpha expression in cultured human astroglial cells by dexamethasone and indomethacin. J. Clin. Invest. 87, 1674–1680.

Zaman, K., Ryu, H., Hall, D., O'Donovan, K., Lin, K.I., Miller, M.P., Marquis, J.C., Baraban, J.M., Semenza, G.L., Ratan, R.R., 1999. Protection from oxidative stress-induced apoptosis in cortical neuronal cultures by iron chelators is associated with enhanced DNA binding of hypoxia-inducible factor-1 and ATF-1/CREB and increased expression of glycolytic enzymes, p21(waf1/cip1), and erythropoietin. J. Neurosci. 19, 9821–9830.

ELSEVIER

Journal of the Neurological Sciences 252 (2007) 57–61

Journal of the Neurological Sciences

www.elsevier.com/locate/jns

Interferon beta-1b exacerbates multiple sclerosis with severe optic nerve and spinal cord demyelination ☆

Yoko Warabi [a,b,*], Yoh Matsumoto [b], Hideaki Hayashi [a]

[a] *Department of Neurology, Tokyo Metropolitan Neurological Hospital, Tokyo, Japan*
[b] *Department of Molecular Neuropathology, Tokyo Metropolitan Institute for Neuroscience, Tokyo, Japan*

Received 13 July 2006; received in revised form 5 October 2006; accepted 10 October 2006
Available online 27 November 2006

Abstract

To evaluate the effect of interferon beta-1b (IFNB-1b) on multiple sclerosis (MS) with severe optic nerve and spinal cord demyelination, we examined the relationship between IFNB-1b treatment outcome and the clinical and genetic characteristics of three types of demyelinating diseases of the central nervous system, i.e., neuromyelitis optica (NMO), MS and MS with severe optic-spinal demyelination. Japanese MS frequently carried HLA DPB1*0501, which is associated with NMO. MS with DPB1*0501 showed severe optic-spinal demyelination represented by longitudinally extensive spinal cord lesion, blindness and CSF pleocytosis. IFNB-1b treatment did not succeed in these patients because of the increase of optic nerve and spinal cord relapse and other severe side effects. IFNB-1b should not be administered to demyelinating patients with genetic and clinical characteristics mimicking NMO such as HLA DPB1*0501 allele, longitudinally extensive spinal cord lesion, blindness and CSF pleocytosis even if they have symptomatic cerebral lesions as typically seen in MS. The present study strongly suggests that these patients should be diagnosed as having NMO.

Keywords: Neuromyelitis optica; Multiple sclerosis; Interferon beta-1b; Longitudinally extensive spinal cord lesion (LESL); Blindness; CSF pleocytosis

1. Introduction

Interferon beta-1b (IFNB-1b) treatment was reported to be effective for Japanese multiple sclerosis (MS) patients [1]. However, in Japan, there are a considerable number of MS patients with very severe optic nerve and spinal cord demyelination mimicking neuromyelitis optica [2,3]. Neuromyelitis optica (NMO) was defined as an inflammatory demyelinating disease in the central nervous system (CNS) in which the lesions are localized in the optic nerve and spinal cord [4]. Conversely, diagnostic criteria for MS only include patients who have cerebral lesions without a long spinal cord lesion extending over three vertebral segments and CSF pleocytosis [5]. Therefore, patients with cerebral demyelinating lesions accompanied by longitudinally extensive spinal cord lesion and CSF pleocytosis were not classified as either NMO or MS, according to the previous diagnostic criteria. Recently, revised diagnostic criteria for NMO were published [6,7]. Autoantibodies called NMO-IgG taken from North American and Japanese NMO patients were reported to stain the perivascular and pial structures of the brain tissue [8,9], and the clinical characteristics of NMO-IgG-positive patients have been partially characterized [10]. However, appropriate treatment for such borderline patients remains difficult because the therapeutic strategy for NMO is different from that for MS.

In the present study, we hypothesized that IFNB-1b treatment is not effective for MS patients with severe optic nerve-spinal demyelination because these patients have genetic and clinical characteristics mimicking NMO. Based on this hypothesis, we retrospectively analyzed the clinical and genetic features of NMO, MS and borderline patients and examined the relationship between clinical and genetic phenotypes and the effects of IFNB-1b treatment. Consequently, we concluded

☆ Sources of support in the form of grants: this study was supported in part by Grants-in-Aid from the Tokyo metropolitan government and the Ministry of Education, Culture, Sports, Science and Technology, Japan.

* Corresponding author. Department of Neurology, Tokyo Metropolitan Neurological Hospital, 2-6-1 Musashidai Fuchu, Tokyo 183-0042, Japan. Tel.: +81 42 323 5110; fax: +81 42 322 6219.
E-mail address: ywarabi@tmnh.fuchu.tokyo.jp (Y. Warabi).

0022-510X/$ - see front matter © 2006 Elsevier B.V. All rights reserved.
doi:10.1016/j.jns.2006.10.008

that IFNB-1b treatment rather exacerbated the clinical status of such borderline patients with cerebral demyelinating lesions accompanied by the NMO-specific HLA allele, DPB1*0501, longitudinally extensive spinal cord lesion, CSF pleocytosis and blindness.

2. Patients and methods

2.1. Patients

We evaluated a series of patients admitted to the Department of Neurology, Tokyo Metropolitan Neurological Hospital, Japan, between August and December 2003, and followed these patients until March 2006. At the time of admission, twenty-seven patients demonstrated clinically confirmed demyelinating disease in the CNS and had shown two or more separate attacks involving the cerebrum, spinal cord or optic nerve that were not attributable to other diseases. During the follow-up period, eight neurologists in our hospital examined each patient regularly and one of the study neurologists (YW) reviewed all medical records after the follow-up period.

2.2. Diagnosis

We diagnosed NMO ($n=12$) based on three "absolute criteria" from Wingerchuk's first diagnostic criteria that require optic neuritis, acute myelitis and an absence of evidence of clinical disease beyond the optic nerve or spinal cord [4]. The presence or absence of "supportive criteria" that include longitudinally extensive spinal cord lesion (LESL), CSF pleocytosis and severe optic neuritis is not considered for the diagnosis.

We diagnosed MS patients ($n=15$) according to McDonald's criteria. These patients had two or more demyelinating attacks including symptomatic cerebral lesions. Abnormality on "paraclinical tests" including LESL and CSF pleocytosis is not discussed for the diagnosis. We classified MS patients to one of the two clinical courses of MS: relapsing-remitting MS (RRMS) or secondary progressive MS (SPMS) after the follow-up period [11]. Eight patients had RRMS, seven had SPMS.

LESL was defined as hyperintensity over a length of three or more vertebral segments on T2-weighted sagittal images with a 1.5 T MRI scanner. CSF pleocytosis was defined as over 50 cells/μL. Severe optic neuritis was defined based on sequelae of bilateral or unilateral complete blindness. After the follow-up period, we reviewed all of the 27 patients' medical records and MRI images preserved in our hospital including those obtained before August 2003, and determined the presence or absence of these NMO-like characteristics in each patient.

2.3. Determination of the presence of HLA DPB1*0501 or DRB1*1501 alleles

Consent was obtained from all subjects tested and the study was approved by the Institute Review Board. Fifteen milliliters of heparinized blood was drawn from 25 of 27 patients at the time of admission as well as from 36 healthy control subjects, then peripheral blood lymphocytes (PBL) were isolated using the density gradient method. RNA was extracted from PBL using RNAzol B (Biotecx Lab, Houston, TX) or TRIzol (Invitrogen, Tokyo, Japan). cDNA was synthesized using reverse transcription with ReverTra Ace-α (Toyobo, Osaka, Japan). The presence or absence of the DPB1*0501 or DRB1*1501 alleles in PBL samples was determined according to the protocol in the 13th International Histocompatibility Workshop. For the determination of DPB1*0501, cDNA was amplified using a DPB1-specific primer pair (5′-GAGAGTGGCGCCTCCGCTCAT-3′ and 5′-GCCGGCCCAAAGCCCTCACTC-3′). Dot blot analysis was performed using the following five digoxigenin-labeled sequence-specific oligonucleotide (SSO) probes; DPB0901 (5′-GAATTACCTTTTCCAGGGA-3′), DPB5503 (5′-GGCCTGAGGCGGAGTACT-3′), DPB6906 (5′-GAGGAGAAGCGGGCAGTG-3′), DPB8503 (5′-AGCTGGACGAGGCCGTGA-3′), and DPB1701W (5′-GAATGCTACCCGTTTAAT-3′). The probes were labeled with digoxigenin using a DIG oligonucleotide tailing kit (Roche Applied Science, Mannheim, Germany). Detection of hybridized probes was conducted with the chemiluminescent signal detection system using CSPD (Tropix, Inc. Bedford, MA, USA).

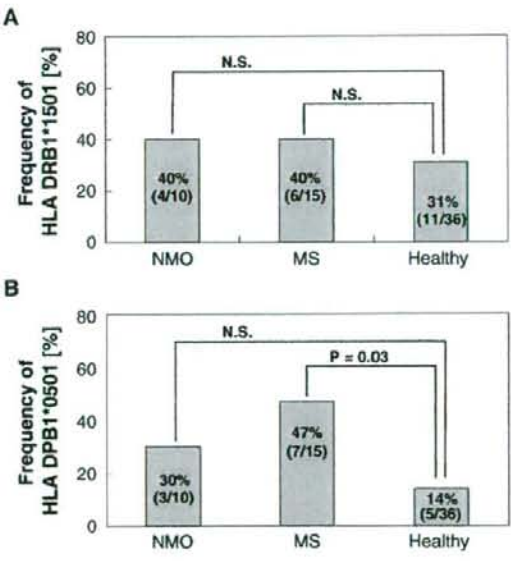

Fig. 1. HLA analysis in 10 NMO and 15 MS, and 36 healthy subjects. (A) Unexpectedly, the frequency of DRB1*1501 allele, which is known as a major HLA allele of MS patients, did not differ between our MS patients and healthy subjects, or between MS and NMO. N.S. indicated not significant. (B) DPB1*0501 allele, which has been reported to be associated with NMO, was carried significantly more frequently by the MS group than by healthy subjects ($p=0.03$).